

UNIVERSIDAD CARLOS III DE MADRID

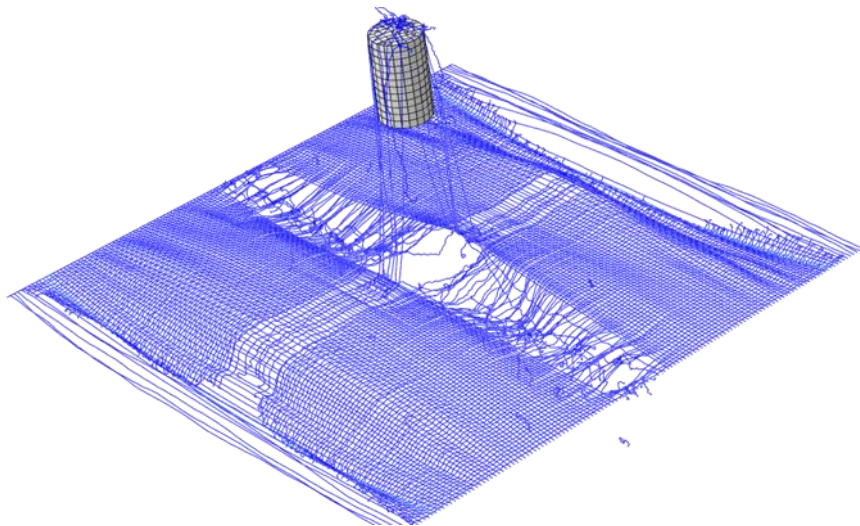
# NUMERICAL STUDY OF BALLISTIC EFFECT AT LOW VELOCITY IN PARA-ARAMID FABRIC

---

## SENIOR THESIS

**Author: Carlos Torija de Diego**

**Tutor: Norberto Feito Sánchez**



Department of Mechanical Engineering



**I want to thank my family for the support provided during these years, and my tutor,  
who has successfully guided me through this senior thesis.**



# Table of contents

|  |    |
|--|----|
| List of illustrations.....                                     | 3  |
| List of tables .....   | 5  |
| 1. Introduction .....  | 7  |
| 1.1. Motivation .....  | 7  |
| 1.2. Objectives .....  | 8  |
| 1.3. Socio-economic impact and ethics.....                     | 9  |
| 2. Kevlar Aramid Fiber .....                                   | 11 |
| 2.1. Properties .....  | 12 |
| 2.2. Comparison with other materials .....                     | 13 |
| 3. State of the Art .....                                      | 15 |
| 3.1. Membrane model vs. yarn fabric model.....                 | 17 |
| 3.2. Energy absorption calculation.....                        | 17 |
| 3.3. Percentage of bullet breakthrough: V0, V50 and V100 ..... | 18 |
| 3.4. Ballistic standards.....                                  | 18 |
| 4. Model implementation.....                                   | 20 |
| 4.1. Introduction to Abaqus version 6.12 .....                 | 21 |
| 4.2. Abaqus units.....   | 22 |
| 4.3. Bullet modeling .....                                     | 23 |
| 4.4. Fabric modeling.....                                      | 26 |
| 5. Results analysis.....                                       | 32 |
| 5.1. Model validation .....                                    | 32 |
| 5.2. Different variable influence in the results .....         | 34 |
| 5.2.1. Bullet shape .....                                      | 34 |
| 5.2.2. Two-sided support .....                                 | 37 |
| 5.2.3. Two fabric layers.....                                  | 44 |
| 5.2.4. Bullet size .....                                       | 45 |
| 6. Operating expenses.....                                     | 48 |
| 7. Conclusions and improvement proposals .....                 | 50 |
| 8. Areas for further investigation .....                       | 51 |
| 9. Bibliography.....   | 52 |
| 10. Appendix .....   | 54 |



## List of illustrations

|  |    |
|--|----|
| Illustration 2.1 Strain test comparison for different yarns [2] .....  | 13 |
| Illustration 2.2 Experimentally obtained stress-strain curves for warp yarns [1] .....                               | 14 |
| Illustration 3.1 Left: Filament level in multi scale model [11]; Right: Multi scale scheme from [10] .....           | 16 |
| Illustration 4.1 Final shape of the flat-nose bullet .....   | 24 |
| Illustration 4.2. 2-D sketch of the round-nose bullet .....  | 24 |
| Illustration 4.3 Flat-nose bullet mesh .....   | 26 |
| Illustration 4.4 Round-nose bullet mesh .....  | 26 |
| Illustration 4.5 Smallest repeatable sequence of fabric .....  | 27 |
| Illustration 4.6 Fabric of dimensions 101.6 x 101.6 mm .....   | 27 |
| Illustration 4.7 Flat-nose bullet with one layer fabric assembly .....   | 28 |
| Illustration 4.8 Round-nose bullet with one layer fabric assembly .....  | 29 |
| Illustration 4.9 Flat-nose bullet double layer detail .....  | 29 |
| Illustration 4.10 Four-sided clamped edges .....   | 30 |
| Illustration 4.11 Detail of initially intended mesh with 7 nodes yarn-to-yarn and final mesh used with 4 nodes ..... | 31 |
| Illustration 5.1 Flat-nose validation chart .....  | 32 |
| Illustration 5.2 Round-nose validation chart .....   | 33 |
| Illustration 5.3 Flat-nose bullet penetration into a fully clamped Kevlar layer .....                                | 34 |
| Illustration 5.4 Middle cross failure and yarn push-aside .....  | 35 |
| Illustration 5.5 Break mechanism timeline scheme for round-nosed case .....  | 35 |
| Illustration 5.6 Energy absorption comparison between flat-nose bullet and round-nose bullet .....                   | 36 |
| Illustration 5.7 Flat-nose bullet penetration in two-sided clamp Kevlar layer .....                                  | 37 |
| Illustration 5.8 A: Yarn uncrimping; B: edge displacement due to yarn uncrimping .....                               | 38 |
| Illustration 5.9 Load vs. displacement of yarn pull-out as obtained from [1] .....                                   | 39 |
| Illustration 5.10 Yarn pull-out at the edge .....  | 39 |
| Illustration 5.11 Complete yarn rip out .....  | 40 |
| Illustration 5.12 Break mechanism timeline scheme for flat-nosed case .....  | 40 |
| Illustration 5.13 Round-nose bullet penetration in two-sided clamp Kevlar layer .....                                | 41 |
| Illustration 5.14 Detail of yarn push-aside before breaking .....  | 41 |
| Illustration 5.15 Break mechanism timeline scheme for round-nosed case .....   | 42 |
| Illustration 5.16 Velocity variation after impact for flat and round cases .....                                     | 42 |
| Illustration 5.17 Energy absorption comparison for flat and round cases .....  | 43 |
| Illustration 5.18 Velocity variation after impact for flat and round cases .....                                     | 44 |
| Illustration 5.19 Energy absorption comparison for flat and round cases .....  | 45 |
| Illustration 5.20 Velocity variation after impact for flat and round cases .....                                     | 46 |
| Illustration 5.21 Energy absorption comparison for flat and round cases .....  | 46 |
| Illustration 8.1 Future investigation, four corner clamping design .....   | 51 |





## List of tables

|   |    |
|---|----|
| Table 2.1 Typical properties of Kevlar aramid yarns [2] .....                                 | 12 |
| Table 4.1. Units used for the finite element model .....                                      | 23 |
| Table 4.2 Bullet dimensions .....   | 23 |
| Table 4.3 Warp and fill yarn material properties [1] and adjusted within margins of error ... | 28 |
| Table 5.1 Validation error .....  | 33 |
| Table 5.2 Third phase curve elasticity and slope, for one layer, fully clamped .....          | 37 |
| Table 5.3 Third phase curve elasticity and slope, for one layer, two-sided clamp.....         | 44 |
| Table 5.4 Third phase curve elasticity and slope, for two layers .....                        | 45 |
| Table 5.5 Third phase curve elasticity and slope, for increased bullet size .....             | 47 |
| Table 6.1 Operating expenses .....  | 48 |
| Table 6.2 Computers life expectancy and cost per hour .....                                   | 48 |
| Table 6.3 Abaqus licence estimation data .....  | 49 |
| Table 10.1 NIJ Standard-0101.06: Ballistic Resistance of Body Armor [14] .....                | 54 |



# 1. Introduction

The need for heavy protection is clear since the apparition of metallic Roman armor, or heavy Middle-Age armors. Nevertheless, they were also difficult to walk with and they weighted more than desirable. Over time, the protection fabrics can provide has improved, using new materials lighter and more difficult to tear. There are many applications where a high-resistant fabric is highly valued, such as in windsurf flags, aerospace compounds or industry workers gloves and suits, among others.

This type of protection has been and will continue being an important subject in weaponry industry. In it, weapon designers try to break through the piece of protective cloth, and, on the other side, bulletproof vest designers making it as tough as possible.

Kevlar is one of the new materials used in the industry with the intention of protecting the person inside the vest and improving it as much as it is feasible. The manufacturing of this material and the size of the yarns give different properties to the final woven material. For this reason, researches in the field are focused on studying different configurations in order to improve the energy absorption in a para-aramid fabric.

The use of numerical tools is very convenient in the study and understanding of this kind of projects, reducing experimental time and money for the companies. At the same time, work with this type of tools, allow to have more control under the different variables that take part in the process.

## 1.1. Motivation

In the research and understanding of Kevlar under impact loads, numerical models represent an important tool in the field. There are several reasons for companies and investigators to take advantage of them over only experimentation. Firstly, their great capacity for controlling variables both precisely and instantly: Young's Modulus, yield stress, friction coefficients and bullet velocity are only a handful of key parameters that can be easily modified. In addition, there exists the possibility of introducing variables out of the scope of regular experimentation: ideal supports, unmanufactured bullet shapes, extremely high impact velocities and others. In addition, the model can repeat simulations consistently, as well as slow them down if required.

Nonetheless, these advantages come at a price. To be able to reproduce the intricate geometry of fabrics and their breaking mechanisms, 3D numeric models reach extreme complexity and computational cost, taking long time to finish a single simulation. However, it is known that 1D fabric models have lower computational cost than their 3D counterparts.

With the intention of making a valid simplified model, capable of predicting fabric behavior under low velocity impacts with reduced computational time, a simplified 1D model is presented. In this study, the influence of bullet shape and size, number of layers and different clamp configurations are analyzed. Therefore, companies can benefit from the aforementioned advantages and obtain fast results in low velocity impact cases.

## **1.2. Objectives**

The senior thesis is created and managed with the main purpose of designing and developing a para-aramid fabric model that will allow simulations of bullet impact in said piece of fabric. In order to achieve this purpose, the model will be implemented by using Abaqus software, which is a program that can perform simulations by means of Finite Element Method, a numeric method to obtain approximate solutions to very complex problems.

As a result, the model is supposed to produce accurate results close to what a real life experiment would provide. To ensure so, the created model will be validated against the literature developed by Das, Jagan, Shaw and Pa [1]. They worked on the influence of inter-yarn friction coefficient, finding a limiting value to obtain the best results.

Once the model is validated, the project will move to investigate how fabric performs in different scenarios. There are several variables that will be tested with special regard, being one of them the geometry for the bullet. In the same way, diverse clamping supports or adding more layers should have an effect in bullet impact.

Under those various circumstances, it is expected to obtain different breakage mechanisms, and diverse degrees of energy absorption and residual bullet velocities.

In order to achieve the aforementioned objectives, a clear and concise methodology has been needed. The methodology had to be precise enough to cover the whole process including possible unexpected results, but open enough to allow changes and alternatives when required. Thus, the next enumeration lists the steps followed in chronological order during the project:

1. Previous research of existing literature related to Kevlar fabric, its properties and bullet impact under different conditions. That will provide the data necessary for the model, such as friction coefficients and material properties.
2. Take into account the necessary assumptions and considerate several simplifications where possible, to make feasible the computations and still maintain the solutions as relevant as possible.
3. Development of an impact model in Abaqus contemplating the two previous steps.

4. Validation of the model by comparing the results obtained with experimental data taken from literature researched in the first step. This phase involves trial and error until the desired results are obtained.
5. Study of the effect of different variables in the model that will provide further knowledge on the breaking mechanism and the energy absorption.
6. Improvements proposal from the study based on the results obtained.

To conclude, the main objective is stated, the validation reference is exposed and the steps to follow are set.

### **1.3. Socio-economic impact and ethics**

This document addresses a subject of great interest in the military field. Although armies perform many investigations with large R&D budgets, usually they are not publicly detailed. The discoveries are maintained secret seeking a competitive advantage. Therefore, there is an important barrier when looking for literature explaining and evaluating the socio-economic impact.

Despite the theoretical approach of this senior thesis, there are some direct applications fields. The bulletproof vest industry is the main one: police officers, security guards and special forces are the most benefitted.

Many engineering researches and inventions must be subjected to an ethical evaluation. That determines the legitimacy of the investigation and justifies the continuity of the project.

Military advancements can generate susceptibilities because their applications are linked to the combat field. Elements such as nuclear bomb, combat aircraft or landmines are tools designed to harm and cause destruction. To put it differently, weapons are used by a person against another one, violating the self-integrity right of the opponent. Thus, it is necessary an after the fact judgement to determine the righteousness of their employment, dependent on the prudence of the actuator.

Nonetheless, this study is focused in reinforcing the security a piece of Kevlar cloth can offer. The main objective of these fabrics, whether they are used in bulletproof vests or in tents to diminish the effects of the enemy fire, is to protect the user. Weaved Kevlar is used in self-defense. That is considered a right and does not interfere with the opponent's self-defense right or any other of his rights. Therefore, an after the fact judgement is not required, and taking into account the previously exposed it can be stated that their use is legitimate.

To conclude, this study is carried out with the intention of contributing to the defense of life, the protection of people, and facilitating the performing of humanitarian tasks in conflictive regions, as well as the rest of the areas where it may be found useful in the future.

## 2. Kevlar Aramid Fiber

The Kevlar Aramid Fiber, which is the material chosen for the project, is the aramid fiber composition for Du Pont company. The fabric official name results of linguistic compounding, where the type of material (Aramid Fiber) and the company name (Kevlar®) are linked for designing a new term. Concerning the semantics, the meaning is a mixture of both elements. On the one side, the *aramid fiber* definition varies according to the source consulted. For this work, it has been selected the explanation provided by the US Federal Trade Commission, which states that it is “a manufactured fiber in which the fiber-forming substance is a long chain synthetic polyamide in which at least 85% of the amide linkages are attached directly to two aromatic rings” [2]. At the same time, Kevlar® was the assigned term for the poly-para-phenylene terephthalamide of the company Du Pont.

The origin of the material dates of the 60's decade, when the researches of the scientist Stephanie L. Kwolek (1923-2014 [3]) allowed the company Du Pont to foresee the creation of fibers with ultra-high young modulus. After many experiments, the first fiber achieved a tensile modulus of 400 gpd (grams per denier). Then, it started the long process of refining the production of the aramid fiber, something that took many years and attempts. In order to manufacture weaved products, fibers need to be adhered to each other creating a yarn, and depending on this process, results in higher or lower denier. The latest term, denier, refers to the weight of the yarn, and is expressed in mass in grams per 9000 meters of yarn.

$$1 \text{ denier} = \frac{1g}{9000 \text{ m}} = 1.1 \cdot 10^{-4} g/m$$

It was not until 1971, when production level grew enough for the building of the first production plant. The final result was the mentioned fiber, which was commercialized as Kevlar.

Later on, other companies have also produced para-aramid fibers with other commercial names such as Twaron®, Technora® or Gold Flex®. Nonetheless, the company responsible for the original discovery, Du Pont, maintains its production and commercialization, being the most widespread and presenting the highest sales figures.

At this point, the material created by Du Pont company was chosen over the rest based on two main reasons. Being the first product of its kind provided prolific papers and investigations from early dates, protecting the development from stagnating if lack of information occurred. Secondly, being a widely used fiber results in easier access to the product and more opportunities to apply the knowledge gained.

## 2.1. Properties

Kevlar fabrics are popular for their excellent mechanical properties: its Young modulus can exceed 80 GPa and present an ultimate tensile strength over 3 GPa. According to some literature, Kevlar KM2 can also stretch 3.5% [1], but higher stretching (5+ %) has been reported [4] before failure. Those properties make Kevlar very capable for mechanical energy absorption and a very desirable fiber to work with. Certain of those properties can be checked in Table 2.1 for the several existing variations:

| Yarn properties                       | Kevlar and Kevlar 29 | Kevlar 49 | Kevlar 68 | Kevlar 119 | Kevlar 129 | Kevlar 149 |
|---------------------------------------|----------------------|-----------|-----------|------------|------------|------------|
| Tensile strength <sup>a</sup>         |                      |           |           |            |            |            |
| gpd                                   | 23.0                 | 23.0      | 23.0      | 24.0       | 26.5       | 18.0       |
| Kpsi                                  | 420                  | 420       | 420       | 440        | 485        | 340        |
| Initial modulus                       |                      |           |           |            |            |            |
| gpd                                   | 550                  | 950       | 780       | 430        | 750        | 1100       |
| Mpsi                                  | 10.3                 | 17.4      | 14.4      | 8          | 14         | 21         |
| Elongation, %                         | 3.6                  | 2.8       | 3.0       | 4.4        | 3.3        | 1.5        |
| Epoxy impregnated strand <sup>b</sup> |                      |           |           |            |            |            |
| Tensile strength, Kpsi                | 525                  | 525       | 525       | 610 est.   |            | 500        |
| Initial modulus, Mpsi                 | 12                   | 18–19     | 16        | 16 est.    |            | 25–26      |
| Elongation, %                         | 4.4                  | 2.9       | —         | —          |            | 1.9        |
| Density                               |                      |           |           |            |            |            |
| g/cm <sup>3</sup>                     | 1.44                 | 1.45      | 1.44      | 1.44       | 1.45       | 1.47       |
| lb/ft <sup>3</sup>                    | 89.9                 | 90.5      | 89.9      | 89.9       | 90.5       | 91.7       |
| Moisture regain, %                    |                      |           |           |            |            |            |
| 25 C, 65% RH                          | 6                    | 4.3       | 4.3       | —          | —          | 1.5        |

<sup>a</sup>Yarn properties determined on 10 in twisted yarns (ASTM D-885).

<sup>b</sup>Strand properties determined on untwisted epoxy-impregnated yarn (ASTM D-2343).

Table 2.1 Typical properties of Kevlar aramid yarns [2]

It is also worthy to mention that Kevlar not only exhibits outstanding mechanical properties, but they are also relatively temperature independent up to the glass transition temperature and can be used up to 250°C.

Currently, eight main types of Kevlar are commercialized [5]:

- Kevlar® AP
- Kevlar® 29 (K29)
- Kevlar® 49 (K49)
- Kevlar® 100
- Kevlar® 119
- Kevlar® 129
- Kevlar® KM2
- Kevlar® KM2 Plus

From this list the most widely used fibers are Kevlar® 29 (K29) and Kevlar® 49 (K49). Kevlar® 29 is the basic original product, as obtained after the manufacturing process. It is oriented to create ropes and shielding outfits, among others. On the contrary, Kevlar® 49 is



intended to create fiber-reinforced composites, receiving surface improvements for an enhanced attachment to the matrix, as well as for optical fiber cables, providing a flexible protection.

The one used in this document is Kevlar® KM2, which is advertised to be specially designed for “meeting performance requirements for helmets and vests for military and high-performing UD’s for spall liners”.

## 2.2. Comparison with other materials

The fact that Kevlar is so widely used in the industry for mechanic intensive requirements can be better understood when compared to some other materials. To keep in perspective the properties of Kevlar, the Illustration 2.1 shows some stress-strain experiments for different yarns.

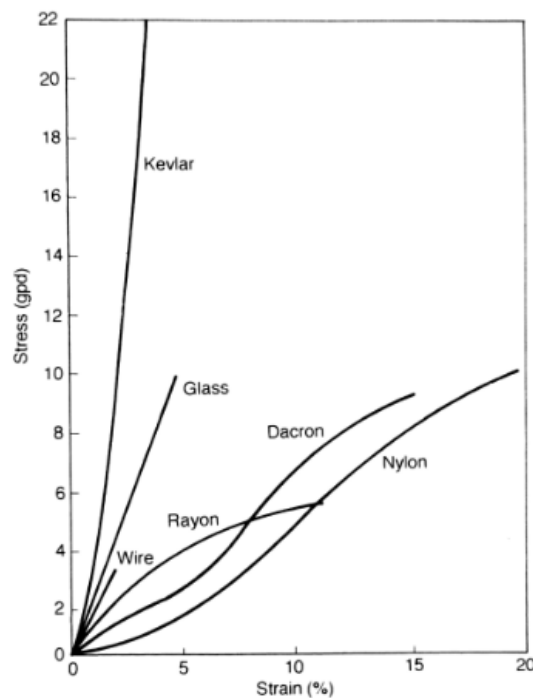


Illustration 2.1 Strain test comparison for different yarns [2]

Kevlar stands out in two important parameters. Firstly, the steeper strain curve that Kevlar provides ensures increased stiffness and increased energy absorption over the same amount of deformation. Secondly, the higher yield stress conveys that fewer yarns will be needed to obtain the same yield force. The yield strain is relatively low, usually under 6%, and commonly ranging from 2 to 4% depending on the type of Kevlar.

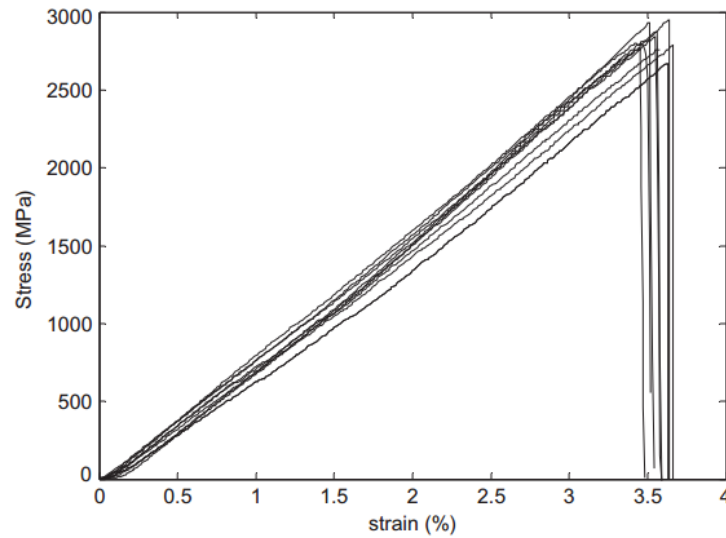


Illustration 2.2 Experimentally obtained stress-strain curves for warp yarns [1]

As it can be appreciated in the set of experiments from Illustration 2.2, the yarns do not present plastic deformation, but a linear behavior up to the breaking point. The implications are that yarns are either broken or working as intended. However, it reduces the amount of energy absorbed and completely eliminates the possibility of hardening through deformation during manufacture.

### 3. State of the Art

Since bulletproof vests have had interest for the industry, there have been different types of investigations and researches related to ballistics. Considering para-aramid fabric excellent properties it is unsurprising its extensive use protective gear. Hence, it is possible to find literature from other authors that study bullet impact on Kevlar fabrics. The next paragraphs present the main contributions in the field.

In 1977, David Roylance publishes a paper [6] in which carries out an analytic analysis of the wave propagation phenomenon. When studying Kevlar fabrics, the most important parameter to find is the critic velocity at which the fabric breaks. He provides the next equation for it:

$$V = \sqrt{\epsilon_0 k E \left[ 2\sqrt{\epsilon_0(1 + \epsilon_0)} - \epsilon_0 \right]}$$

Where:

- $V$  is the critic velocity
- $\epsilon_0$  is the maximum stretching value produced by the impact
- $E$  corresponds to the material Young modulus
- $k = 88260$  is an unit conversion factor

Nevertheless, in the same paper it is pointed that the wave propagation problem magnitude surpasses the analytic mathematical methods. For a more in-depth investigation, it is necessary a numerical analysis, which leads the way to Finite Element Method field.

The Finite Element Method (FEM) is a numeric analysis that relies on the discretization of the real problem. As a consequence, it is a simplification of reality, and as such, the results are an approximation to the actual ones. As detail and model complexity grow, the more accurate the results will be. On the contrary, increasing the level of detail of simulations has severe scaling problems. Not only computationally, as it demands increasing processing power, memory and time, but also in terms of deeper knowledge as new variables become relevant.

The first level of detail on FEM fabric modeling is the creation of a continuum membrane that replicates the properties of Kevlar. It is the least computer intensive approach and yields the fastest results. Using it, Zhijiang et al. [7] simplified a 3D angle-interlock weave composite into cubic cells using a VUMAT subroutine. They reported that although successful, not considering the microstructure level failure entails low precision results.

The next level models yarns as 1D elements. Compared to the membrane model, this second grade complexity stage allows for several benefits, which are discussed on the immediate following section. In 2005, following the 1D weaved scheme and including a

viscoelastic behavior, V.B.C. Tan et al. [8] showed it was possible to obtain accurate results of residual velocities for high velocity impacts ranging from 100 m/s to 500 m/s. More recently, in 2014, Das. et al. [1] investigated inter-yarn friction, concluding that increasing values beyond a certain limit would result in reduced impact performance.

With the aim of increasing the accuracy, the next step includes modeling yarns as 2D bands. The model made by C. Ha-Minh et al. [9], belongs to this category. In it, it was possible to see fabric damage mainly from lateral yarn movement. Also, its model reported broken yarns related to fixed ends and pull-out corresponding to free edges.

In case further detail is needed, yarns can be modeled as 3D elements or even as groups of filaments. It allows for very precise simulation of contact among yarns, fiber deformation under impact, yarn section change and partial yarn breakage. Nevertheless, it comes at the cost of elevating the computing tax considerably. To achieve a good compromise for accuracy and compute time G. Nilakantan et al. [10] proposed a convenient multi scale solution where the impact region uses 3D solid elements and shell elements elsewhere. Subsequently, Gurav Nilakantan [11] further refined the multi scale up to filament level as shown on Illustration 3.1. His model showed that filament lateral mobility influences ballistic performance. On the contrary, it did not affect the projectile deceleration, wave propagation nor yarn internal energy variation.



Illustration 3.1 Left: Filament level in multi scale model [11]; Right: Multi scale scheme from [10]

Progressively increasing the level of detail is only one trend of replicating real life experiments. When performing ballistic experiments to validate the model, the need to include probabilistic effects on the model arises. Thus, the critic velocity is replaced by V50 (further details are discussed on section 3.3). Deterministic FEM cannot replicate the variability on the experimental results. A solution is proposed by Nilakantan [12] slightly modifying the properties of each yarn that receives the impact. An unexpected result was reported: increasing the standard deviation decreased V50, suggesting that weaker yarns had higher influence than stronger ones.

Finally, fabric researches are also concerned about testing conditions: clamp support configuration, several layers, and bullet shape or size lie inside this category.

### 3.1. Membrane model vs. yarn fabric model

On the attempt to reduce the computational time of Kevlar impact models, two main simulation levels are found on literature: a continuum membrane with the same properties as a detailed fabric, or a discrete fabric composed by hundreds of yarns. This later one has been the selected modeling method due to several reasons.

Although very compute efficient, membrane models cannot replicate certain low level phenomenon such as slippage and yarn unraveling [8]. Yarns are not tied one to another but connected by a contact surface. This contact surface will provide friction force whenever one yarn is stretched or moved aside. Bullet impacts will be the cause of yarn movement, so it can be expected friction to play a sizable role during the process. An impact in a yarn with higher friction regarding the surrounding yarns will present higher yarn recruitment, thus, spreading the impact over a wider area.

If a yarn breaks in the clamp support due to the impact, or some other previous circumstance, it is still beneficial. Apart from preventing the rest of the yarns to move aside, it can unravel and the slippage will keep dissipating energy. Bullets with a perforating prone shape, such as cones, spheres, oval-shaped or any other variation, can also push aside the yarns along their movement and make easier their way through the fabric.

The previously mentioned effects cannot be addressed in a continuum membrane model. Therefore, this kind of approach would restrain the investigation and would not be suitable for testing these types of bullets, which is why a one dimensional bar element yarn fabric is chosen.

### 3.2. Energy absorption calculation

There are two main strategies in order to minimize the damage from a projectile. The first of them is to deflect it. That requires the protective layer to present a hard and slippery contact surface and the impact should be angled so the bullet deviates from its original trajectory. Both requirements are not met by the Kevlar model, therefore the importance of the second strategy: maximize energy absorption.

The energy absorbed by an impact is the sum of the deformation energy of the yarns, the kinetic energy that acquires the fabric and the temperature increase due to the friction during yarn sliding [13]. This process is out of the scope of this study. Instead, the Charpy test principles will be used. The Charpy test is based on the fact that the energy absorbed corresponds to the work done by the external forces. By extension, that is, to the difference between the initial mechanical energy and the remaining one after the impact. The mechanical energy is defined by the formula:

$$E_{mechanic\ initial} = E_{mechanic\ final} + E_{absorbed}$$

$$E_{mechanic} = E_{kinematic} + E_{potential}$$

Usually, the Charpy test interchanges the kinetic energy and the potential energy. In the study case there is no potential energy variation, thus, the difference will be computed as the difference of the kinetic energy of the bullet. The next expression is obtained:

$$E_{absorbed} = \frac{1}{2}m_{final} \cdot v_{final}^2 - \frac{1}{2}m_{inicial} \cdot v_{inicial}^2$$

Where:

- a)  $m$  represents the mass of the bullet, before the impact ( $m_{inicial}$ ) and after the impact ( $m_{final}$ ).
- b)  $v$  is the velocity of the bullet, before the impact ( $v_{inicial}$ ) and after the impact ( $v_{final}$ ).

Knowing there is no partial detachment of bullet material, nor adhesion of the yarns to the bullet, it can be considered that the initial mass and the final mass remain the same (7.5 g). Leading to the next conclusion:

$$E_{absorbed} = \frac{1}{2}m \cdot (v_{final}^2 - v_{inicial}^2)$$

### 3.3. Percentage of bullet breakthrough: V0, V50 and V100

When employing FEM, only one parameter is used to determine penetration success or failure: critic velocity. On the contrary, when dealing with experimental data it is necessary to account for probabilistic effects. This variation responds to uncontrollable variables such as young modulus and yield stress of yarns not being uniform.

The term V0 refers to the maximum velocity at which the projectile has no probability of trespassing the fabric. Thus, it is the maximum safe impact velocity for a certain type of bullet and conditions. Usually, the breaking success-failure is expressed in a Gaussian distribution. If the impact velocity is increased, the fabric is no longer safe, and when 50% ratio is achieved, V50 is reached. It is important to emphasize that it is not an acceptable security standard. On the contrary, V100 designs the minimum velocity at which a complete penetration is certain.

### 3.4. Ballistic standards

In the ballistic field, there are different military standards for rating gear. Some examples are the US standard, named Mill STD 662 E, the UK standard, called UK/SC/5449, or the NATO Standard, named STANAG 2920.

The National Institute of Justice (NIJ) has its own standards, which are the ones used by law enforcement and correction officers in US. The *NIJ Standard-0101.06: Ballistic Resistance of Body Armor* [14] covers gear impact performance when dealing with ballistic threats and it establishes a frame of reference for comparing protection elements. For any of those levels, it requires not only perforation resistance, but also protection against blunt trauma by limiting the impact depth reached. According to this standard, personal armors can be classified in six types of increasing ballistic performance:

- a) Type IIA (9 mm; .40 S&W)
- b) Type II (9 mm; .357 Magnum)
- c) Type IIIA (.357 SIG; .44 Magnum)
- d) Type III (Rifles)
- e) Type IV (Armor Piercing Rifle)
- f) Special Type

Table 10.1 in the *Appendix* provides more details on the required impact performance for each category.

## 4. Model implementation

Making a complete replica of reality would require the simulation of very low order phenomenon reaching up to the atomic scale. This in-depth simulation is not feasible for a couple of reasons, the first being that it would require a very deep knowledge of all the interactions between elements. The second one is related to the fact that with so many elements and interactions involved the computation requirements would increase to limits beyond what current computation can provide, making it an unfeasible task.

To solve this problem and reduce computation times to reasonable limits, it was created a simplification of reality. For its commissioning, it is needed to include the following assumptions:

- a) Yarns are modeled as a series of one dimensional elements. Real experiment yarns are comprised of around 400 filaments that are weaved together. Those filaments will work unitedly when receiving an impact and are not expected to break apart partially. This simplification allows for modeling the yarns as a string made of one dimensional elements, which reduces the computational time and also the complexity of the model implementation.
- b) Bullet will only move in impact direction; all other directions of movement are restrained. The restriction includes rotations, since a rotating bullet after the impact will add unneeded complexity to residual velocities and energy measurements.
- c) Bullet shapes will be limited to regular simple shapes. Real life possible irregularities due to manufacturing imperfections or material not being completely homogeneous lie outside the scope of this project.
- d) Temperature variations are not considered to affect the fabric material or the bullets properties.
- e) Aerodynamic effects are disregarded. This approximation should have insignificant effect as the bullets will be shot as close to the Kevlar® fabric as possible, turning negligible any possible variation.
- f) Gravity is considered to be zero. The mass implementation in the model is considered to obtain the bullet kinetic energy, but no effect will be presented regarding gravity.

These simplifications will have from little to no impact in the final results. Nevertheless, before their acceptance, it must be proven that the model provides results very close to reality. By using Abaqus software, the availability of producing fast model modifications is ensured.



## 4.1.Introduction to Abaqus version 6.12

Abaqus version 6.12 is a highly adaptable commercial Finite Element software that allows creating virtual models with up to extremely high geometry complexity. Consequently, those models can be tested and examined to determine their performance, and their parameters can be modified to match the expectations.

In engineering, it is relatively frequent to face sizable problems with complex geometry to which there is no analytic solution. Nevertheless, it is usually known how to solve the same problem for very simple geometries. Finite Element Method strategy is established around dividing the entire geometry into smaller elements with a shape that is possible to solve. As those simpler shapes normally do not match very precisely the bigger structure, it is necessary to decrease their sizes at their minimum for increased accuracy.

The resolution of a problem with Finite Element Method software undergoes three phases. Abaqus different modules fit within those:

a) Pre-process phase: The pre-process consists on the problem definition itself. Here it is where the model is introduced in the program, taking into account the necessary simplifications. The next modules belong to this phase:

1) Part Module: In this module, the geometries and basic pieces of which the model is comprised are defined. It can be done in Abaqus own editor, although there is also the possibility of importing the geometries from other CAD programs in case of more complex geometries.

2) Property Module: It allows defining the materials of which the created pieces are made. Those materials are assigned to sections, and the sections are assigned to the geometries created in the Part Module.

3) Assembly Module: The assembly module allows placing the pieces defined before in their relative positions in space.

4) Step Module: In this module, the type of analysis that is going to be performed is introduced. It also allows defining the time the simulation will last.

5) Interaction Module: After having placed the different parts in space, it is necessary to establish the relations among them, from joining geometries to set the type of contact between pieces.

6) Load Module: It allows introducing the loads and the boundary conditions for the parts, as well as the restrictions to movements and initial velocities.

7) Mesh Module: It generates the meshes that discretize the model, which is the base for the Finite Element Method. A more refined mesh will contain a greater number of elements, and therefore the results will be more accurate. However, the computation time will increase considerably, which makes necessary to balance the mesh resolution in relation with the bearable margin error and the compute time available.

- b) Processing phase: In this part of the process the simulation of the introduced model is computed. It does not require any input by the user. The computation time depends on the problem complexity and the mesh resolution. It is only comprised by the Job module, in which is established the number of cores used by the processor. It is possible to monitor the evolution of the results and interrupt the process if necessary.
- c) Post processing phase: In the final phase, the user can visualize the results of the analysis and check the evolution of the variables of interest. It is convenient to remind that the model introduced is a simplification of the real phenomenon. Over this simplification it is applied the finite element analysis, which again, is an approximation to the already simplified model. Therefore, results should be examined with a critical eye.

Abaqus also offers additional modules, *Optimization* and *Sketch*, which are not required for this specific problem. The module configuration is expected to change depending on the software brand, but the structure *pre-process*, *process* and *post-process* will remain.

## 4.2. Abaqus units

Before starting with bullet and fabric modeling it is important to warn about setting the basis for the unit system. Along the paper, numerous properties and measures will be given. All of them have their own units, but a quick look to Abaqus interface will suffice for the user to realize there is no unit specified next to the input boxes. This is because Abaqus does not work with concrete units. This is not a choice made by the user but a software design choice.

Thus, the unit system should be coherent. In this case, the basic International System (SI) was not utilized. Two principle arguments support the decision. Initially, it is not suitable for the measurements; and secondly, the measurement units do not coincide with the used ones for the rest of the literature. Therefore, a variation with multiples and fractions has been used, as detailed in the Table 4.1:

| Magnitude | SI                     | Used in Abaqus model     |
|-----------|------------------------|--------------------------|
| Lenght    | m                      | mm                       |
| Time      | s                      | s                        |
| Mass      | kg                     | ton                      |
| Force     | N                      | N                        |
| Pressure  | Pa (N/m <sup>2</sup> ) | MPa (N/mm <sup>2</sup> ) |
| Velocity  | m/s                    | mm/s                     |
| Energy    | J                      | mJ                       |

Table 4.1. Units used for the finite element model

Some users may encounter the situation where the results differ several orders of magnitude from the expected one. In that case they should check the input data, since (in most cases) the units are wrongly introduced.

### 4.3. Bullet modeling

The steps to follow for the bullet modeling, which are the ones mentioned in section 4.1. Specific details are provided for this case.

#### Design

The importance of the bullet design lies on the fact that the bullet nose shape will affect the ability of the bullet to break through the fabric. That nose will either spread the impact over a wider area or help to push aside the yarns, resulting in a less effective fabric. For validation purposes two different shapes are created:

- a) Flat-nose bullet: The flat-nose bullet created for the validation is modeled as a cylinder with the parameters shown in the Table 4.2:

|             |     |
|-------------|-----|
| Radius (mm) | 4.5 |
| Length (mm) | 15  |
| Weight (g)  | 7.5 |

Table 4.2 Bullet dimensions

In spite of its possibility, it is not necessary to use any additional software to import the bullet geometry. As it is a simple geometry Abaqus editor is sufficient. Starting from the plane, a circumference of radius 4.5 mm is created. Then, it is extruded 15 mm along the “Z” axis, to obtain the final shape, on Illustration 4.1.

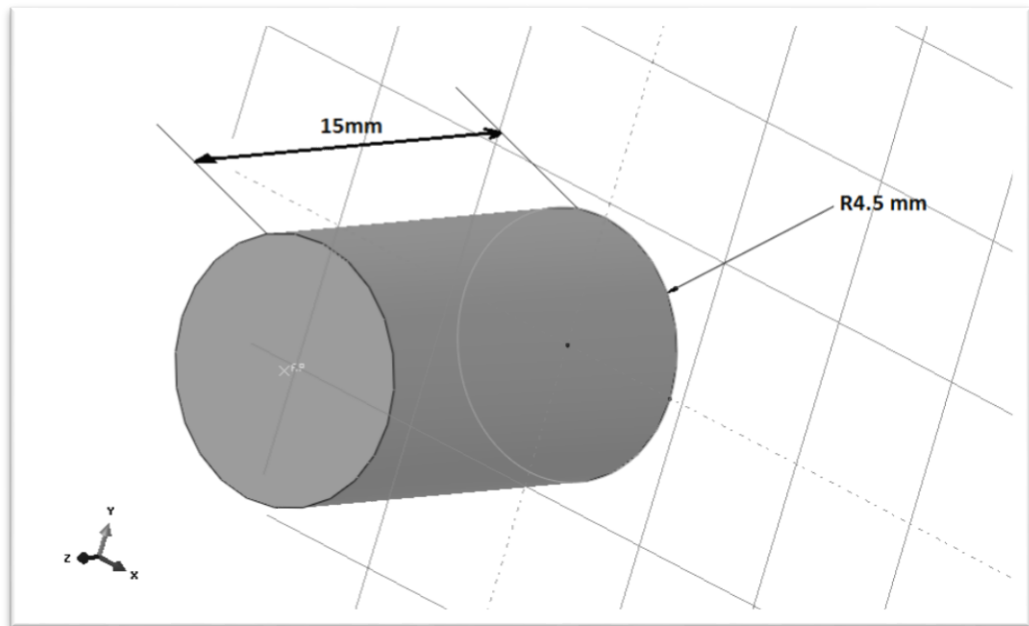


Illustration 4.1 Final shape of the flat-nose bullet

Finally, the flat nose needs to be selected as a surface, to make possible subsequent contacts.

- a) Round-nose bullet: The round nose bullet is created similarly to the previous one. Firstly, the base structure is sketched; and then, the symmetry of the bullet is employed to create a revolution solid, as in Illustration 4.2.

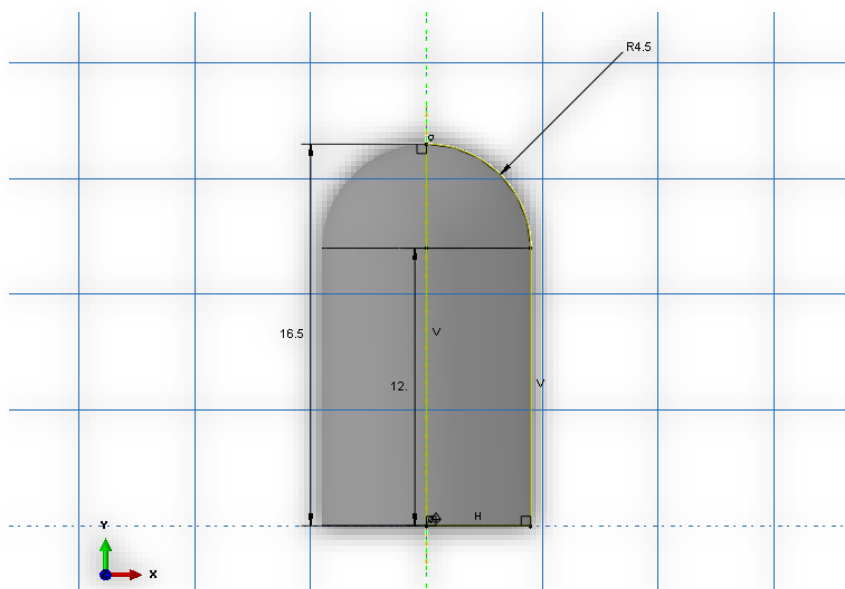


Illustration 4.2. 2-D sketch of the round-nose bullet

As it happened with the flat-nose bullet, the round nose also needs to be selected as a surface, to make possible future contacts.

## **Properties**

When setting the type of object the bullets are, it should be stated as *rigid solid*. There are several reasons for it:

- a) The first motive is that bullet deformation is not taken into consideration. Bullet shape will change during the impact, depending on the material properties. Materials with low mechanical properties will experience significant deformations, losing the original intended shape. On the contrary, materials with high mechanical properties will not undergo a significant deformation, in which case, it is sensible a rigid body assumption. Hence, making the simulation independent from the material provides an ideal scenario which uses an infinitely rigid body.
- b) The second reason is that by doing so, the computing time decreases significantly, since deformations involve numerous compute heavy calculations.
- c) Thirdly, the simulations performed need to be compared to previous simulations made by other researchers. To match previous papers conditions for the validation process, rigid bullet is the preferred option.

This decision implies that no material properties will be assigned, but the bullet weigh. That is 7.5 grams in all of the bullets, independently on what volume they have and what density may yield. This weight is extracted from the reference paper for validations [1].

## **Loading**

As a rigid 3D object contained in a 3D space, a bullet has 6 degrees of freedom. All rotations should be restrained and the “Y” and “X” coordinates should remain constant. The result is an object that can only displace in the direction of the impact. That last degree of freedom will correspond with the bullet velocity towards the fabric and it will be defined before each simulation. The velocities will range from 10 m/s to 120 m/s depending on the case.

## **Meshing**

Bullets meshes are formed by quadrilateral shell elements, named R3D4 on Abaqus. The flat-nose bullet has a node-to-node distance of 0.5 mm. This ensures a top view with a fairly accurate circle resemblance. The total element count is 2437 with 2431 nodes.

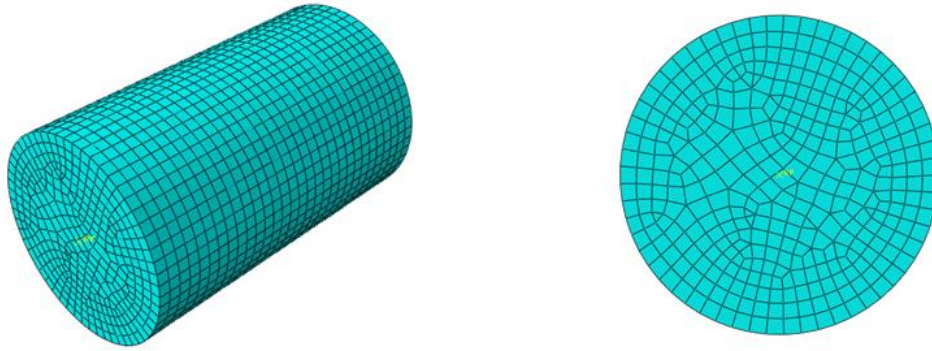


Illustration 4.3 Flat-nose bullet mesh

For the round-nose bullet, the mesh resolution for the nose is as high as the previous bullet, that is, being 0.5 mm between nodes. The rest of the body can use a lower resolution mesh with longer elements of the same thickness, which still preserves the outer circular shape. That yields 739 nodes and 745 elements, with lower numbers than the flat-nose bullet due to bigger elements around the bullet body.

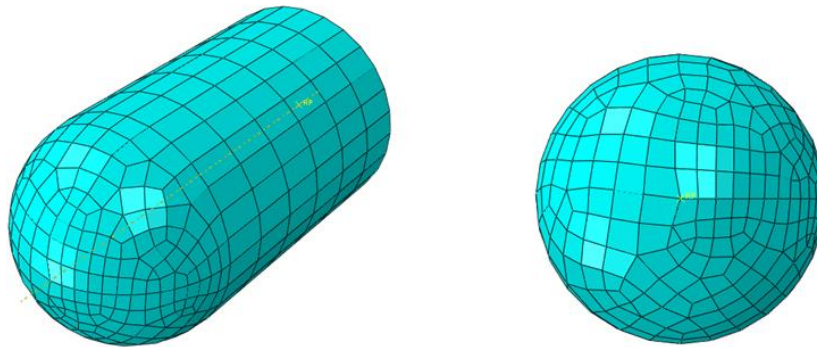


Illustration 4.4 Round-nose bullet mesh

#### 4.4. Fabric modeling

In the following section, it will be described the materials characteristics used for the fabric, the mesh size, properties and conditions, among others. Concerning the main piece of fabric is a 101.6 mm side square fabric. To build this piece of fabric there are several parameters that need to be defined, and these will be introduced in Abaqus along the several steps explained in section 4.1

##### Design

Fabric is composed by unitary cells as shown in Illustration 4.5, measuring 1.494 x 1.494 mm. It should be noted that the yarns form a tri-dimensional shape, passing on top and below one another, and not contained in the same plane.



Illustration 4.5 Smallest repeatable sequence of fabric

At this point it is important to indicate that the yarns have an outer cylindrical surface. That surface should be tied to the geometry to make it independent of the mesh, instead of tied to the mesh, which would prevent from refining the mesh freely.

The creation of the surfaces is performed ahead of time in foresight of the creation of the interactions. The convenience of it lies on the fact that this module will be cloned to archive a 101.6 mm square fabric. That is a 68x68 module matrix like the one in the Illustration 4.6, and if not done now it will cost a lot of time to redo the model.

The creation of this square fabric is a very computer resource demanding task, which should be taken into account.

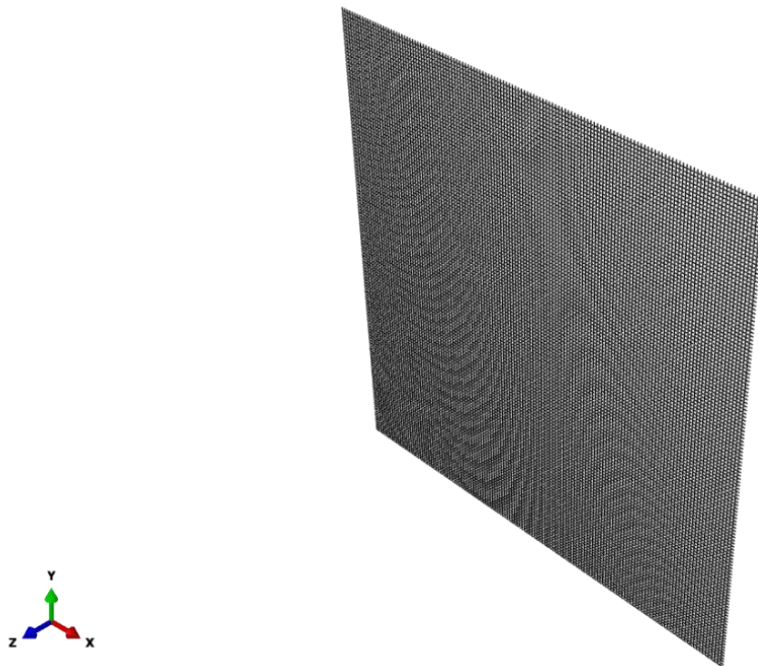


Illustration 4.6 Fabric of dimensions 101.6 x 101.6 mm

## Properties

There are two important issues to address in this module: set the materials and set the sections that will be attached to the yarns.

- a) Materials: The yarns are divided into fill yarns and warp yarns depending on their orientation, presenting each one its own properties. As a result, it requires the creation of two different materials with the data from Table 4.3.

| Property                     | Fill                  | Warp                  |
|------------------------------|-----------------------|-----------------------|
| Density (Kg/m <sup>3</sup> ) | 1.44*10 <sup>-9</sup> | 1.44*10 <sup>-9</sup> |
| Young's modulus (Mpa)        | 83000                 | 67860                 |
| Yield Stress (Mpa)           | 2930                  | 2410                  |
| Fracture Strain (%)          | 0.035                 | 0.035                 |
| Fracture energy (J)          | 51.27                 | 42.17                 |

Table 4.3 Warp and fill yarn material properties [1] and adjusted within margins of error

- b) Sections: The section is considered to be *truss* of an approximate cross section of 0.064 mm<sup>2</sup>, and assigned with the materials already created to the fill and warp yarns.

It is recommended to do these assignments to the small fabric module, and then clone it to the full size in order to avoid repeated user input, resulting in an inefficient user time management.

## Assembly

On the assembly module, the bullets are placed pointing towards the direction of the fabric with a hitting spot right in its center. As there will be three situations tested, three different assemblies are created:

- a) Flat-nose bullet with one layer fabric:

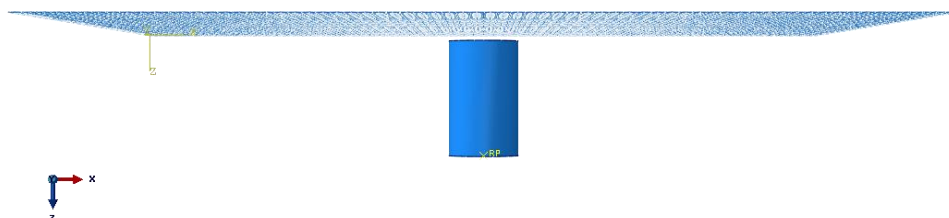


Illustration 4.7 Flat-nose bullet with one layer fabric assembly



b) Round-nose bullet with one layer fabric:

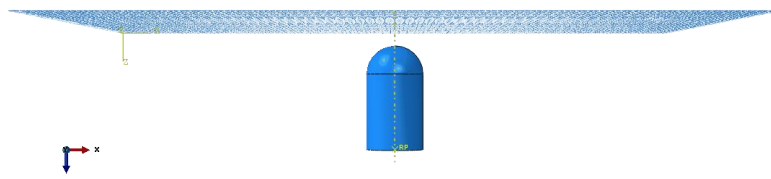


Illustration 4.8 Round-nose bullet with one layer fabric assembly

c) Flat nose with two layer fabric: The two layer simulation has the same element disposition as the one layer assembly, noting that the yarns do not have lateral displacement neither on the “X” axis nor the “Y” axis, only varying the “Z” coordinate. A detailed view can be seen on Illustration 4.9.

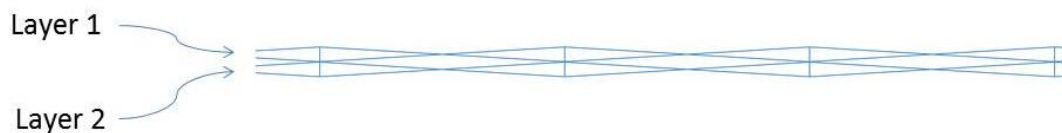


Illustration 4.9 Flat-nose bullet double layer detail

## **Step**

During simulations it is common the need to apply different conditions in different time periods to the model. For example, it could be requested Abaqus to apply a load to our test piece during a certain amount of time, and then remove it and apply some other different load, or temperature variation or any other condition. To allow for this flexibility, the simulation can be divided into several time frames called steps.

The first time step needed is the initial step. It has no time duration, so the actual simulation will not be happening there. However, it is valid to set the initial conditions and be the start point for the next step.

A second time step is created afterwards with the conditions of “Dynamic” and “Explicit”. For the validation case it lasts 8 milliseconds, as this is a time frame big enough to let the bullet hit the fabric, let it deform and get a final residual velocity. This means that further in time there is nothing of interest happening, so setting this step to last longer will incur in more compute time. On the contrary, if set a narrower time frame, like 5 milliseconds, the simulation will not provide a stabilized residual velocity for the slowest paced bullets.

Once the simulation is over it is possible to request Abaqus the evolution of some variables of interest. The frequency at which they are recorded is another factor that influences the compute power needed. For the reference case 200 measures record are requested, spread evenly along the 8 milliseconds.

## **Interaction**

The surfaces of the different elements within the simulation are expected to collide among each other. In this situation Abaqus needs to be specified how it should manage these contacts. The surfaces of the interactions should have been created beforehand in the part module to be able to set the two main interactions in the model:

- a) Bullet-nose to woven contact: The contact will be introduced as two factors: by a normal and a tangential component. The normal component will be defined as a “hard contact” in Abaqus, meaning they both surfaces are solid and one will block the movement of the other. The tangential component has a “Penalty” friction formulation, with a friction coefficient of 0.22 [1].
- b) Woven to woven contact: Likewise, it contemplates the normal component, also “Hard contact”, and the tangential behavior set as “Penalty” with a friction coefficient of 0.19 [1].

## **Loading**

During the experiments the piece of fabric is held with a clamped support which prevents it from moving. As the working space is 3-dimensional, any node will have 6 degrees of freedom. Choosing “Encastre” for all the edge nodes will restrict all those degrees of freedom and keep the fabric tightly held. Setting the boundary conditions is a process that needs to be done on a per-layer basis, so in the case of double layer it should be repeated on both. The final result should look like Illustration 4.10, where the orange coloring represents the restrain of the degrees of freedom.

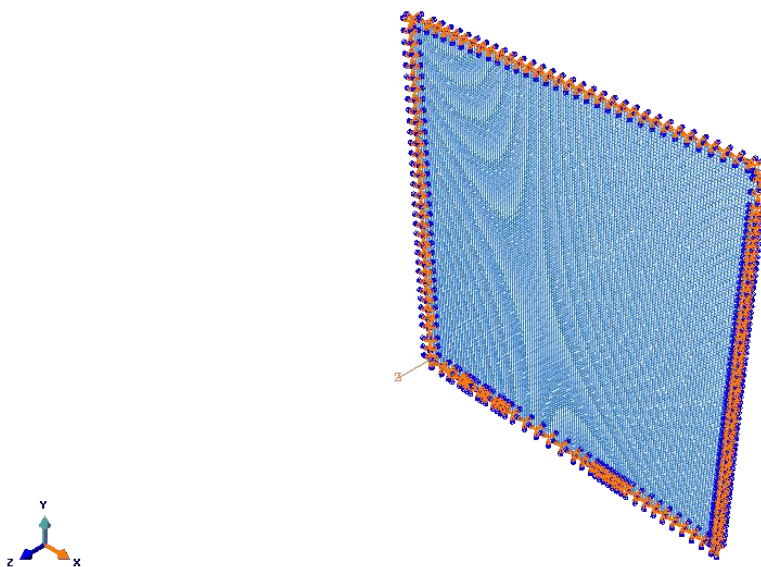
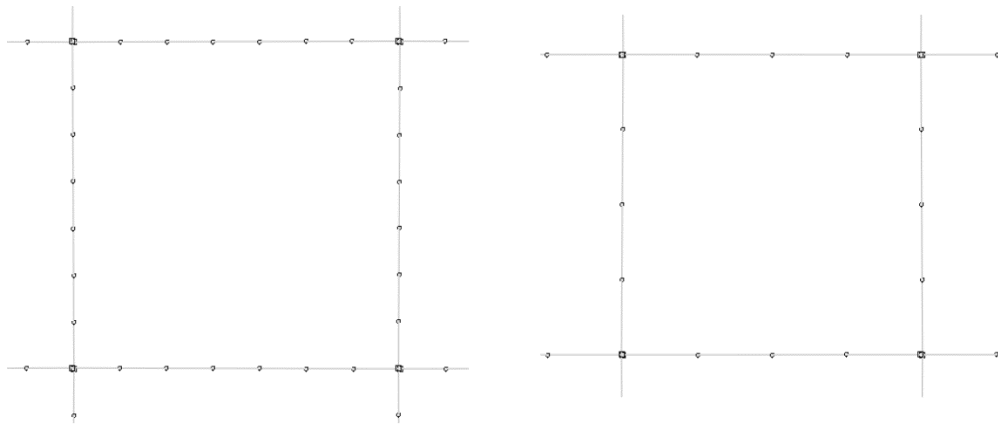


Illustration 4.10 Four-sided clamped edges

## **Meshing**

Since the mesh is composed by 1D yarns, the elements used are *truss* type [1]. Meshing the fabric is a task with very low scalability in terms of computing time. Low nodal meshes can be resolved quite fast by a personal computer. On the other hand, increasing the number of nodes will have a big impact on computing times. Initially, for more accurate results, the fabric was meshed with 7 elements yarn-to-yarn. Nevertheless, due to computation time the mesh resolution had to be scaled down slightly to make feasible the attainment of the results, especially for the two layer configuration. That configuration yields 148,240 nodes and 147,968 elements. Nevertheless, the model still provides accurate values, and further increasing mesh resolution only rises computation times.



**Illustration 4.11** Detail of initially intended mesh with 7 nodes yarn-to-yarn and final mesh used with 4 nodes

## 5. Results analysis

Once the bullet and fabric data are implemented in Abaqus, all the needed settings are introduced and simulations computed, the model is able to yield results. They comprise the validation and the outcome for the new desired conditions.

### 5.1. Model validation

For the model validation a set of impact simulations are performed with the conditions described in the literature [1]. That is using a one-layered fully clamped fabric with square dimensions of 101.6x101.6mm, and bullets ended in flat and rounded surfaces. The model is expected to match the velocity variation of the bullet, which will directly relate to the kinetic energy absorbed by the fabric.

To obtain results close to reality it is necessary to modify the values of the material's constants within the limits provided by Das et al [1]. Their specific values are provided in the previous section. This adjustment must be valid for both cases, flat and round nosed bullet. As a result, the testing process and the value magnitude selection are hindered, because both bullets have different types of breaking mechanisms, as it can be seen in the following section 5.2.1. Illustration 5.1 and Illustration 5.2 show the fitting of both graphs with Das et al. up to a reasonable degree.

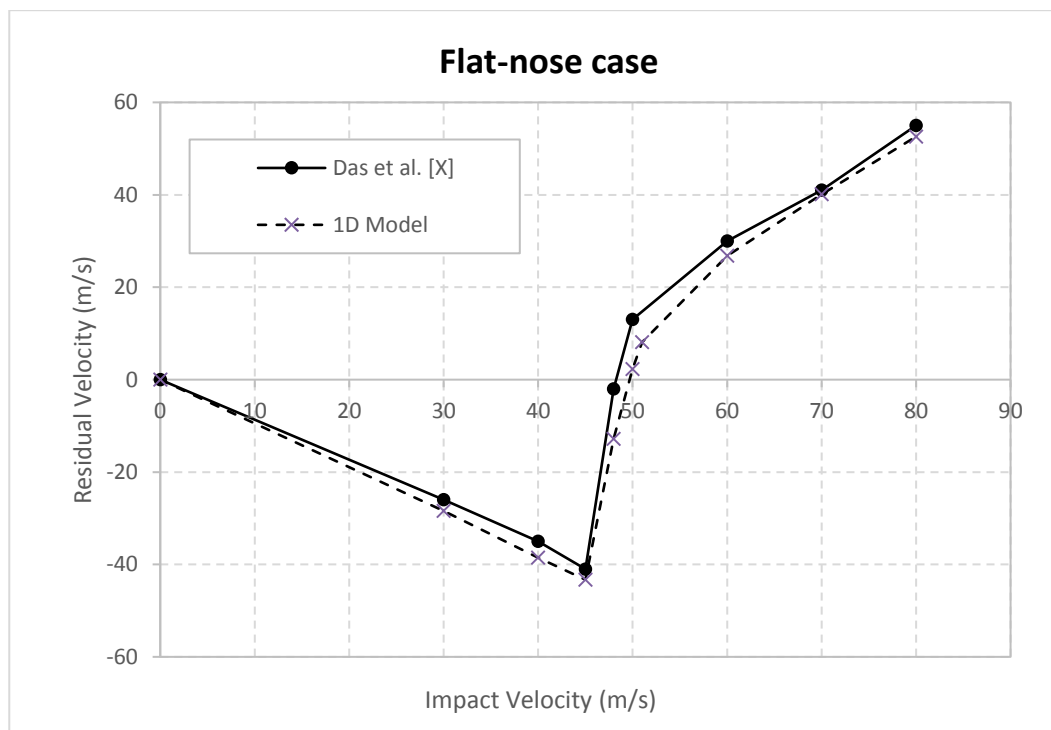


Illustration 5.1 Flat-nose validation chart

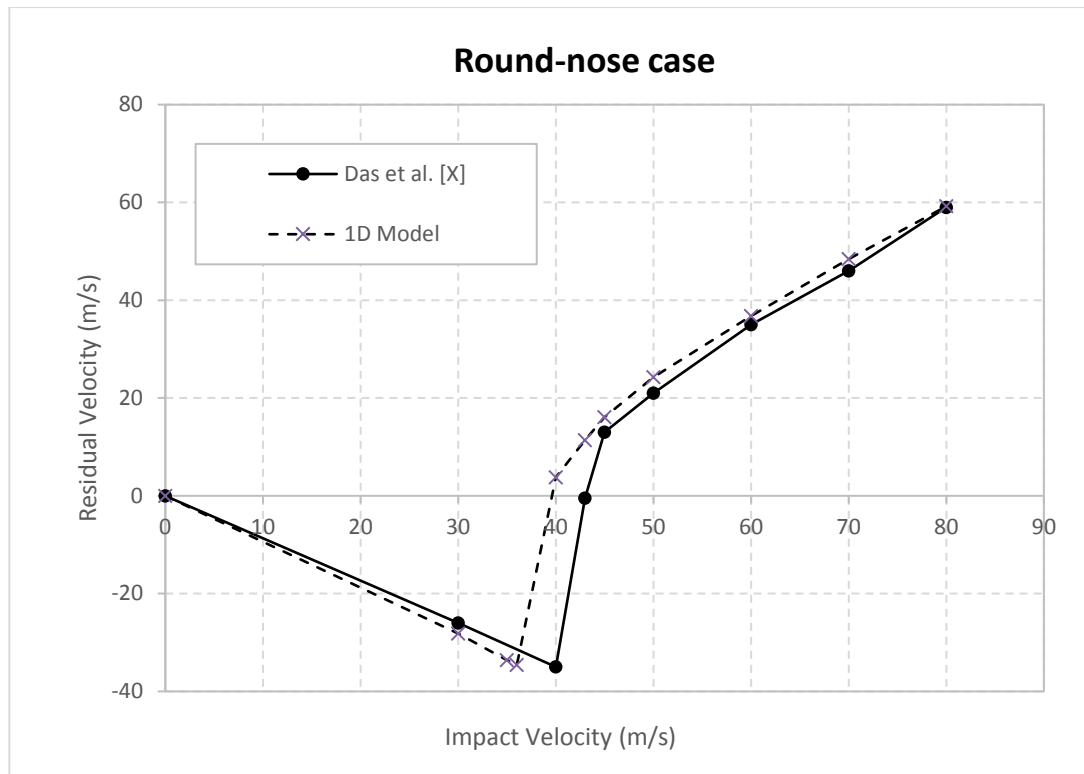


Illustration 5.2 Round-nose validation chart

Paying attention to residual velocities in both simulations, it appears a certain delta in results. Caused by the steepness of the slope, the critic velocities account for the maximum error, which is registered in Table 5.1.

| $V_{critic}$ | Das et al.<br>(m/s) | 1D model<br>(m/s) | Difference<br>(%) |
|--------------|---------------------|-------------------|-------------------|
| Flat case    | 48                  | 50                | 4.1               |
| Round case   | 43                  | 40                | 6.9               |

Table 5.1 Validation error

The fitting of the residual velocities curves and the table above represents the proof of validation of the present model. The model is able to reproduce the trend and values similar to real ones, and the difference with them lies within an acceptable range for this type of numeric study.

This one-layered fully clamped configuration is considered the reference experiment, and it will be the one to which the rest of the results will be compared to.

## 5.2. Different variable influence in the results

Once the model is validated, the fabric can be tested in different conditions to examine its ballistic performance.

### 5.2.1. Bullet shape

Bullet shape supposes an important variable to influence fabric behavior. In the validation process two different shapes were proposed and their differences will be analyzed, along with their break mechanisms and the energy absorbed.

Break mechanism and energy absorption are two linked concepts. Yarn behavior along an impact will directly affect the bullet deceleration, resulting in certain mechanisms being more effective than others. A simple visual inspection would identify those mechanisms. The coloring legend represents the tension that undergoes each yarn, being the reddish colors the ones with greater tension.

#### Flat-nose bullet

In Illustration 5.3 the impact process is shown for the flat-nose bullet. There is only one main mechanism in this case: fiber elongation. Since the bullet contacts the fabric, it recruits a cross of vertical and horizontal yarns that progressively elongate, stopping the impact. As seen on the coloration, the tension distribution on the recruitment cross is fairly even.

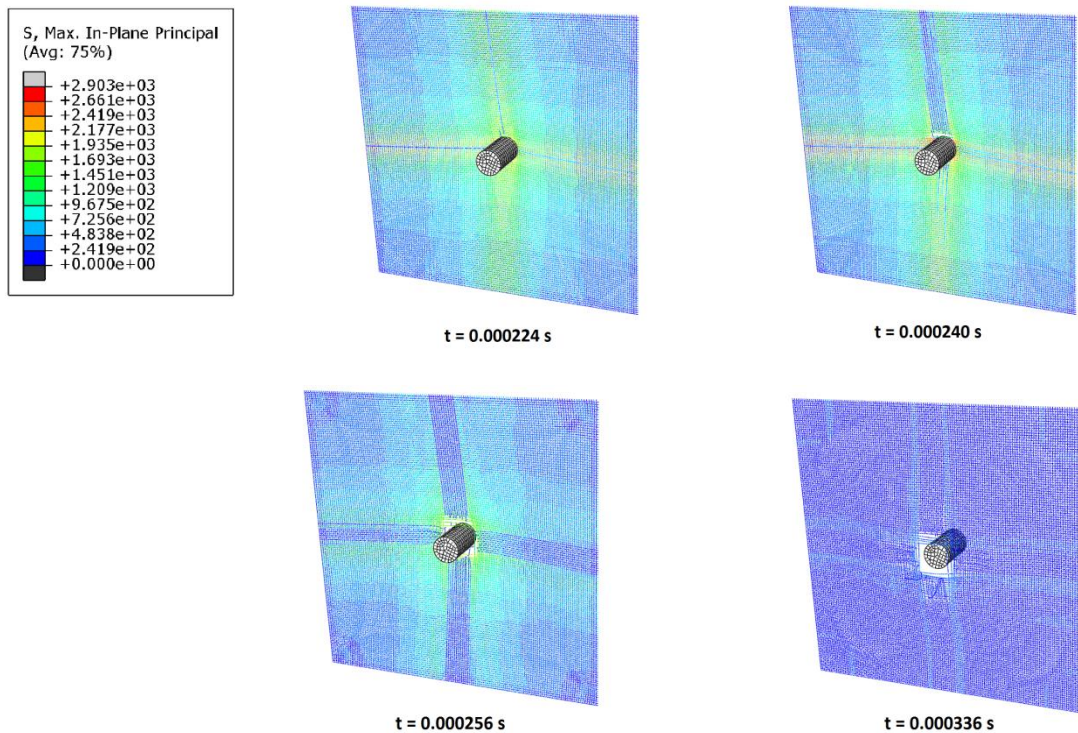


Illustration 5.3 Flat-nose bullet penetration into a fully clamped Kevlar layer

### Round-nose bullet

This scenario is very similar in graphic terms to the previous one. The four edge-clamps guarantee a cross of yarn elongation. Nevertheless, the tension distribution is not even for all of them, since the bullet shape demands higher elongation for the fibers contacting the tip. It will cause the failure of three (fill) and four (warp) central yarns depending on the direction of the fibers.

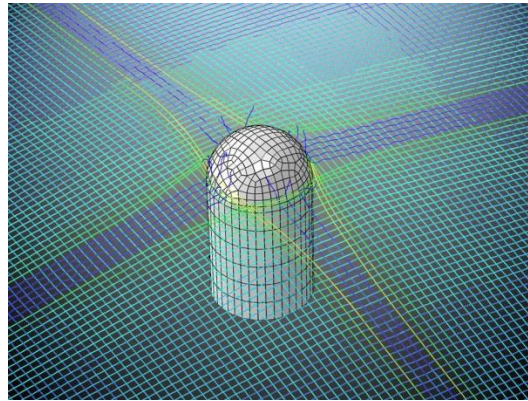


Illustration 5.4 Middle cross failure and yarn push-aside

From then onwards, the broken fibers no longer hold in place the neighbor yarns. Consequently, the rest of the yarns that composed the elongating cross are pushed aside, ending the energy dissipation (Illustration 5.4). Although push-aside is another kinetic energy dissipating mechanism, its effect is small and negates yarn elongation for involved yarns. Thus, the energy absorption is expected to be lower than the flat-nose case. A timeline of the process is shown in Illustration 5.5.

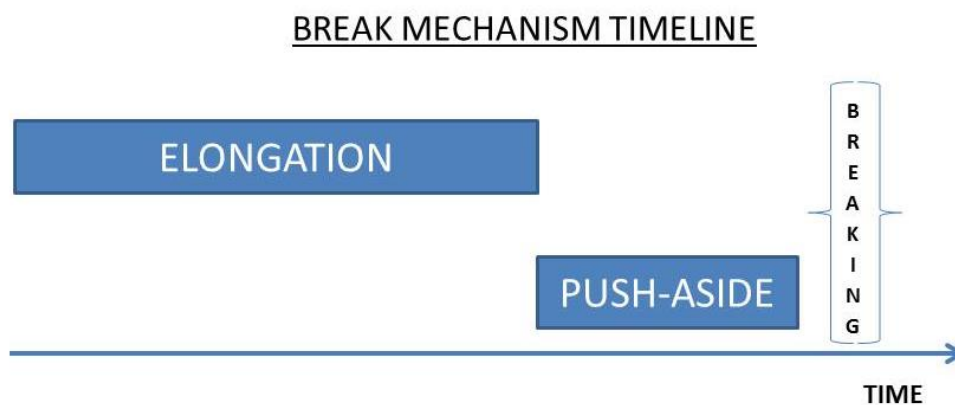


Illustration 5.5 Break mechanism timeline scheme for round-nosed case

Once the resultant velocities are obtained, it is possible to compute the energy absorbed in each impact following the principles of the Charpy test. The graphs of energy absorbed vs.

impact velocity undergo three noticeable stages (Illustration 5.6), which correspond to the velocity variations on the residual velocity versus impact velocity graphs:

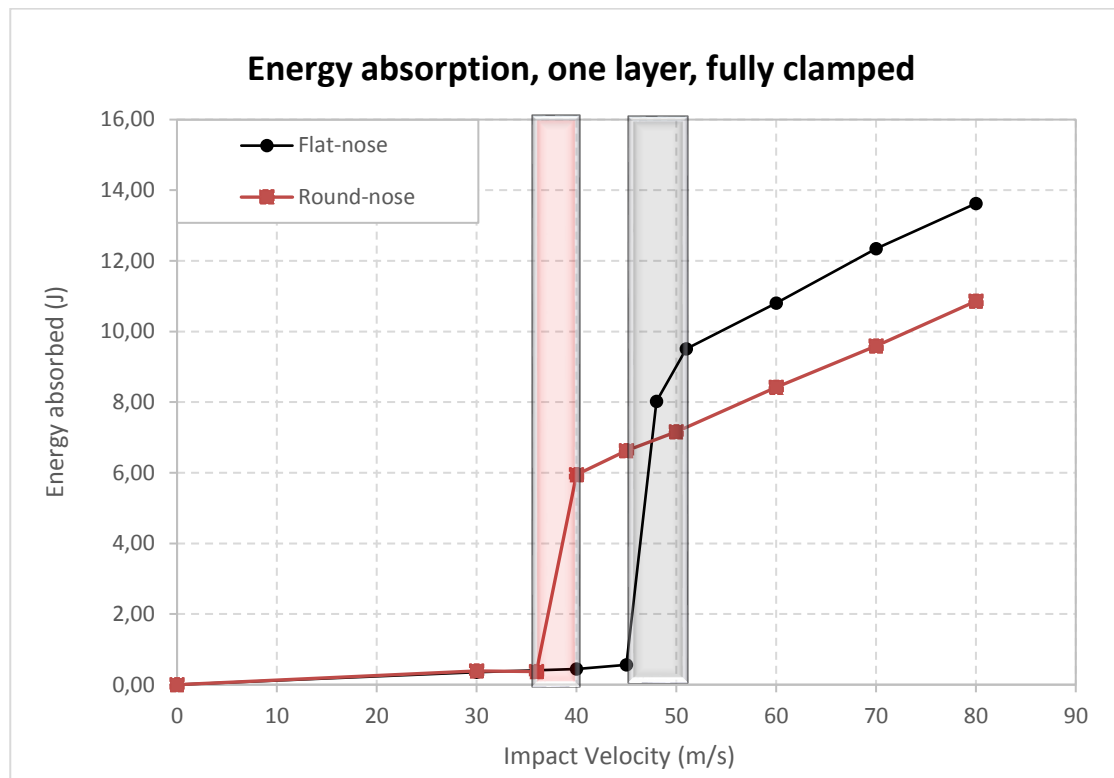


Illustration 5.6 Energy absorption comparison between flat-nose bullet and round-nose bullet

- The first one is a linear behavior with a slight slope. This phase is dominated by fiber elongation. If not surpassed, the yarns will return back most part of the elastic energy stored, acquiring the bullet almost the original velocity towards the opposite direction. Thus, only a small amount of energy is dissipated. It can be appreciated up to the time  $t = 0.000224$  s on Illustration 5.3.
- The second phase is an abrupt increment in absorbed energy, which corresponds with the breaking of the fabric. The yarns surpass their tensile yield stress and collapse, dissipating energy in the process. It can be seen between time  $0.000240$  s and  $0.000256$  s. The cylindrical bullet reaches close to 10 J, while the round-ended stays in 6 J. These regions are marked on Illustration 5.6 with vertical bands.
- If the initial velocity is further augmented, the cloth keeps increasing the dissipated energy. That is because the yarns acquire a greater velocity after the impact, taking it from the bullet. The resultant slope, which sits between the two previous ones, and the curve elasticity are shown on Table 5.2 defining those values the trend of the curve.



|            | Slope<br>( $J \cdot s/m$ ) | Elasticity<br>( $\frac{\% \text{ energy variation}}{\% \text{ velocity variation}}$ ) |
|------------|----------------------------|---|
| Flat case  | 0.149                      | 0.761   |
| Round case | 0.123                      | 0.822   |

Table 5.2 Third phase curve elasticity and slope, for one layer, fully clamped

Although for both cases the same principles apply, the difference in results lies on yarn recruitment. It concentrates the impact in less number of yarns, and that explains the premature entrance on the second phase and the less energy absorbed on it, resulting in earlier breakage.

### 5.2.2. Two-sided support

When moving to a two-sided support, certain differences appear in the results compared to the reference model. The sequence is analyzed for both shapes separately because they present different behaviors.

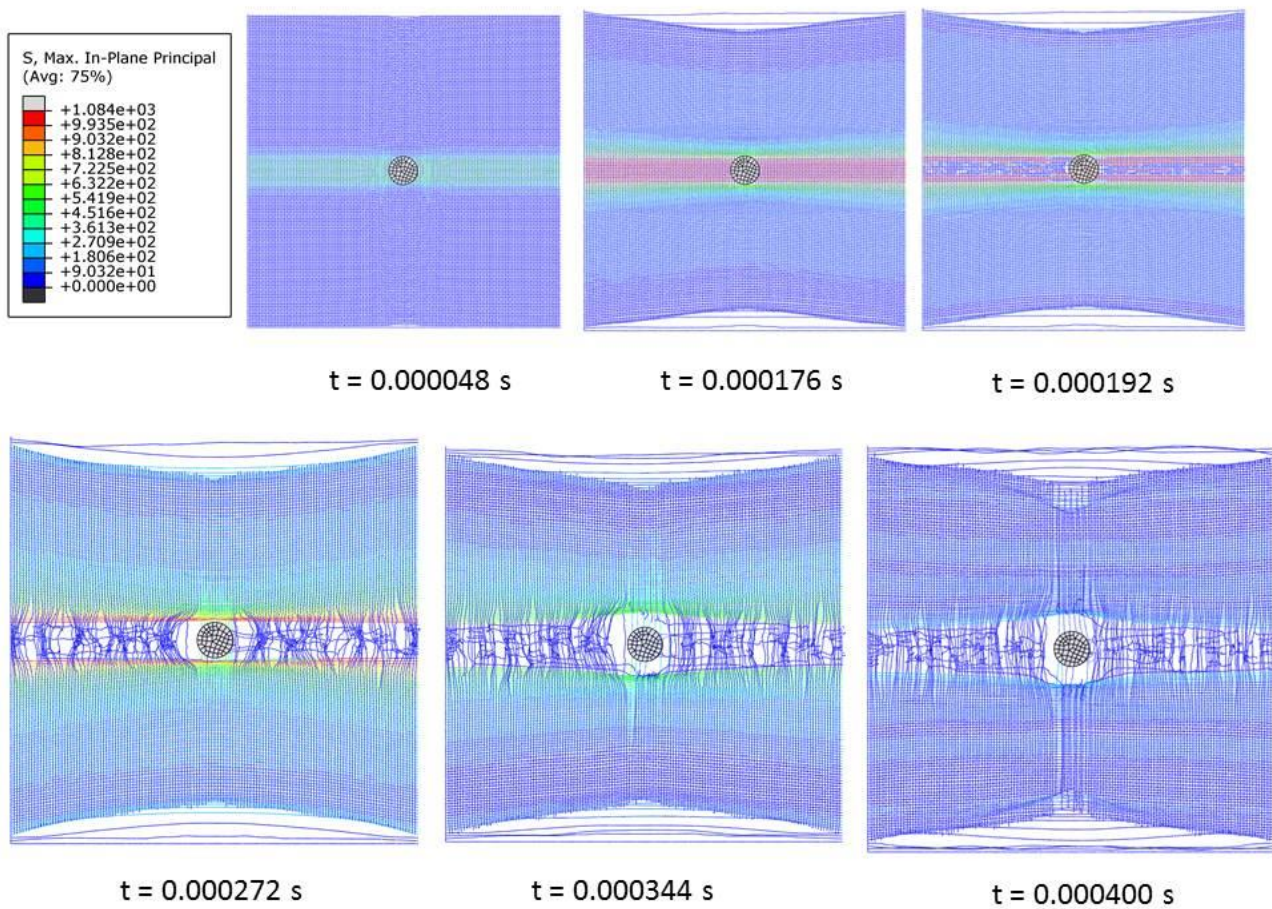


Illustration 5.7 Flat-nose bullet penetration in two-sided clamp Kevlar layer

### Flat-nose bullet

Captures have been taken for distinct moments of the same simulation: from the initial contact to bullet's final velocity. In Illustration 5.7 it is shown the sequence of bullet penetration for the flat-nosed case.

As the horizontal yarns are clamped and the vertical ones are not, there appears three distinct energy absorption mechanisms: elongation, uncrimping and pull-out:

- a) Elongation: When the flat-nose bullet contacts the fabric, and due to the halved support, it generates a middle horizontal band of bullet width. Nevertheless, yarn recruitment does not end in this band. The vertical yarns spread the load progressively resulting in a color gradient towards blue, being the load very small at around a quarter the length of the fabric apart from the impact. This phase provides energy absorption by elongation, and it lasts until  $t = 0.000192$  s. At that moment, the central band reaches its maximum elastic deformation (colored in red).
- b) Uncrimping (or straightening of the yarns): At the same time the vertical yarns straighten and lose their weaved shape. Uncrimping causes the deformation of the unclamped supports (Illustration 5.8). That corresponds to the A-B region of Illustration 5.9, provided by Das. et al. [1].

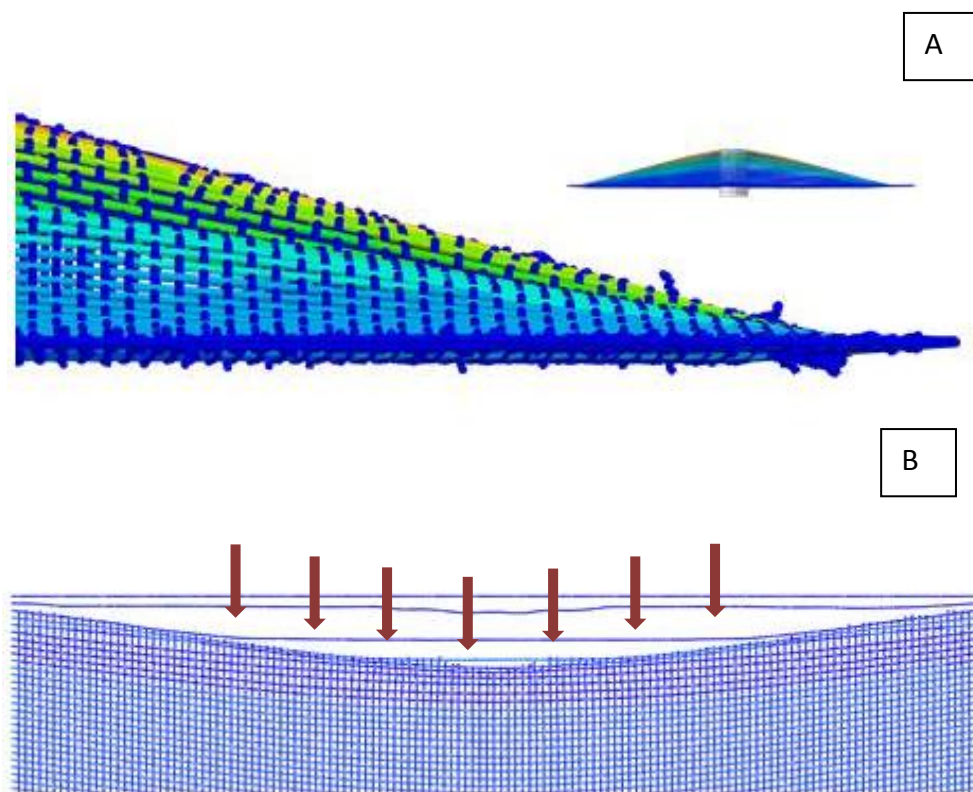


Illustration 5.8 A: Yarn uncrimping; B: edge displacement due to yarn uncrimping

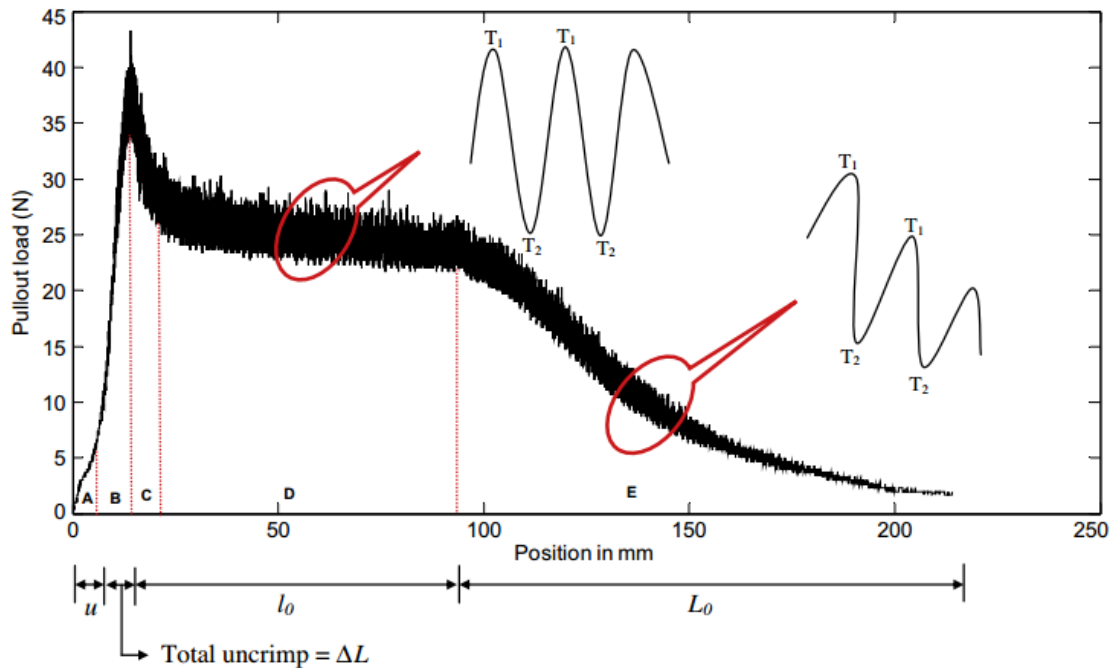


Illustration 5.9 Load vs. displacement of yarn pull-out as obtained from [1]

After this phase, the horizontal fibers cannot increase their elongation and break apart, turning the central band back to a dark blue coloration. The yarn recruitment reaches both upper and lower ends. That means that all the cloth is affected by the impact and collaborates in the impact absorption, although the yarn exploitation is very low compared to said central band.

- c) Pull-out: From this point onwards, the bullet is now only held by the vertical yarns, which are pulled out by the bullet.

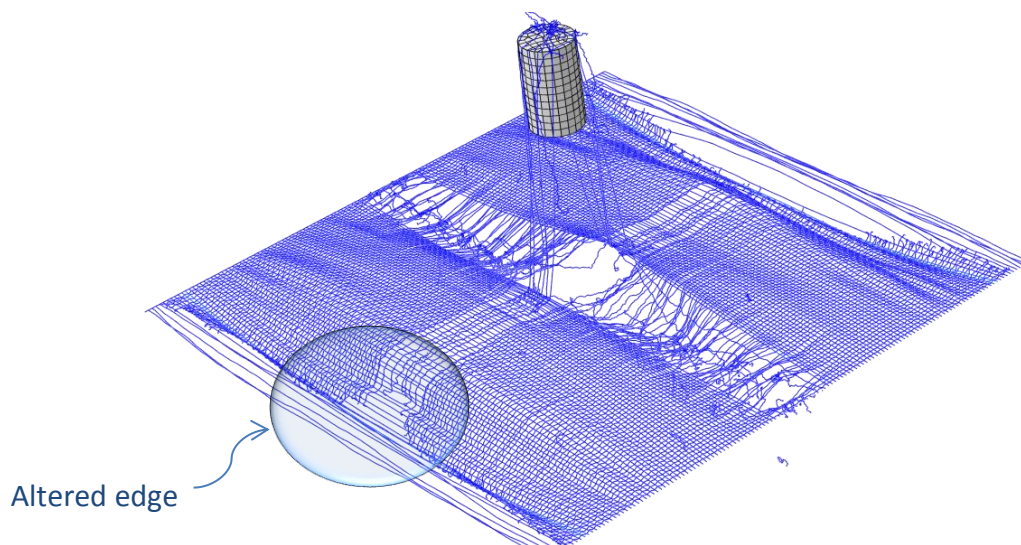


Illustration 5.10 Yarn pull-out at the edge



When yarns are completely extracted from the fabric the final velocity is reached, as there are no further mechanisms to stop the bullet.

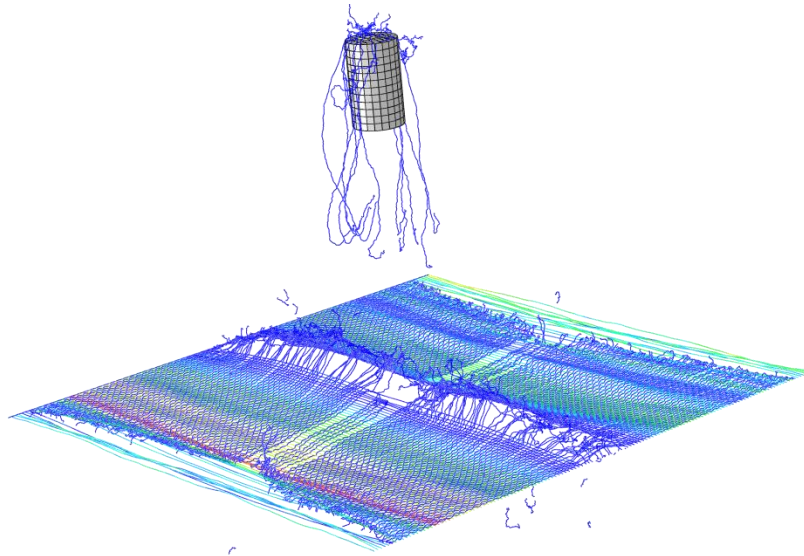


Illustration 5.11 Complete yarn rip out

The resulting timeline scheme is shown on Illustration 5.12.

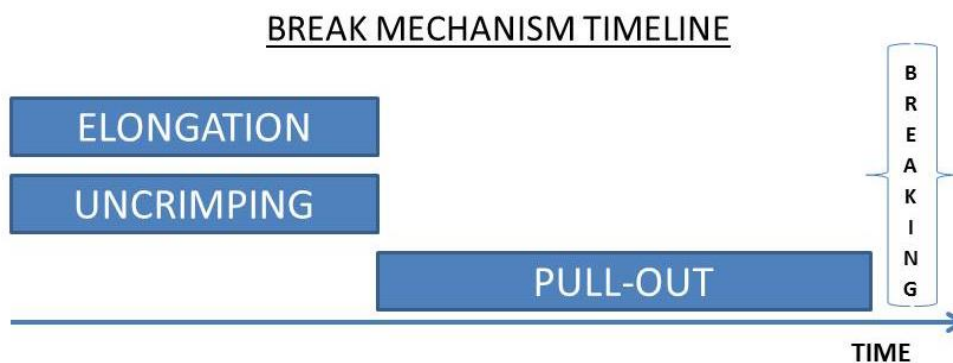


Illustration 5.12 Break mechanism timeline scheme for flat-nosed case

### **Round-nose bullet**

The sequence of impact for a round-nosed model exhibits a different behavior, as seen on Illustration 5.13. In contrast, the main energy dissipators are yarn push-aside and elongation.

- a) Push-aside: When the bullet tip has a rounded shape, the yarns are forced to move to the sides. This process not only absorbs little energy, but also diminishes or even negates the other mechanisms (uncrimping, pull-out and elongation) to a great extent.
- b) Elongation: The central band that supports the greatest part of the impact is very narrow, since part of the middle fibers has been pushed aside. As a result, it is much

smaller than the bullet diameter, only comprised by the three red tinted yarns on Illustration 5.14.

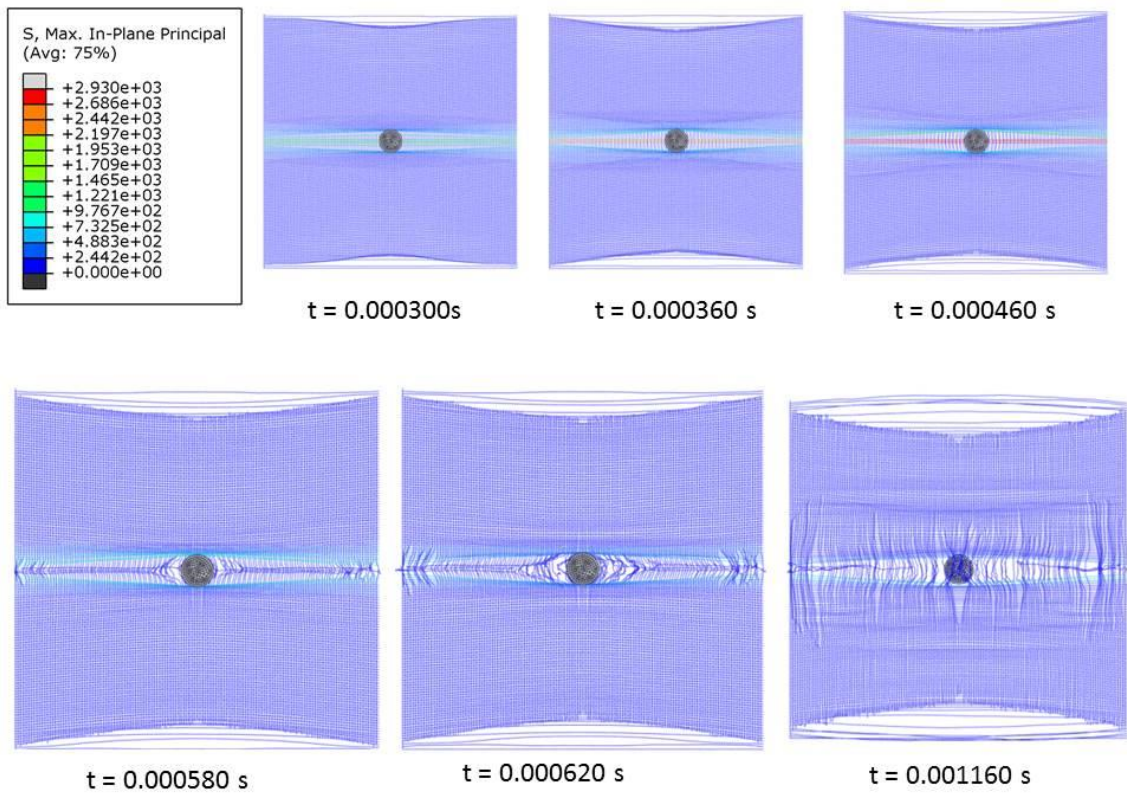


Illustration 5.13 Round-nose bullet penetration in two-sided clamp Kevlar layer

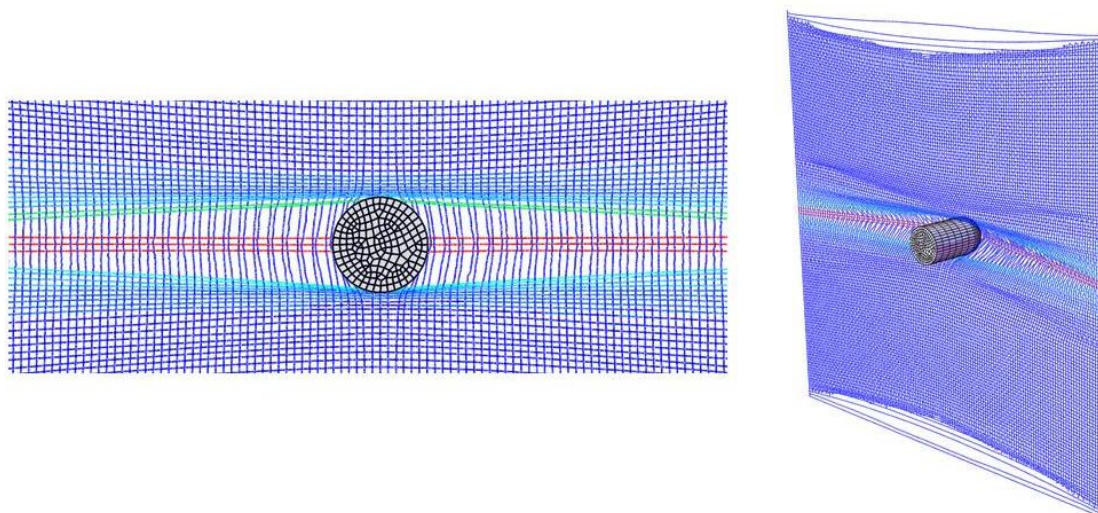


Illustration 5.14 Detail of yarn push-aside before breaking

Moving forward through the simulation, when the bullet acquires its final velocity, all the fabric suffers a light tension. Nonetheless, in general terms it is less affected than the flat-nose case. Illustration 5.15 shows the schematic timeline.

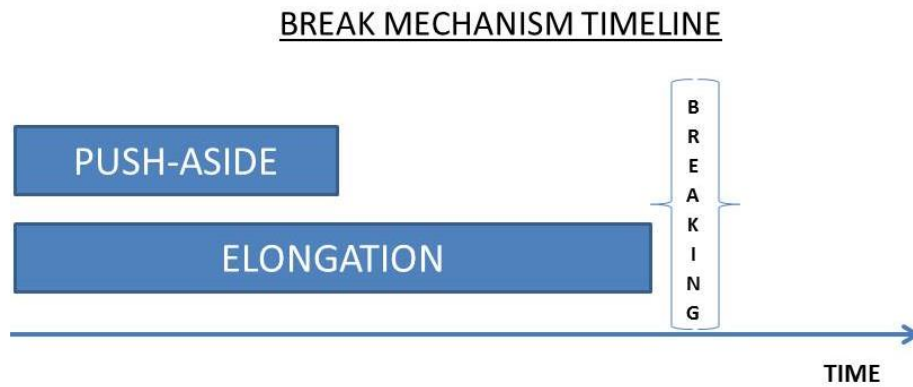


Illustration 5.15 Break mechanism timeline scheme for round-nosed case

Certain differences appear in the results when analyzing the velocity variation. The flat-nosed bullet undergoes an additional phase during the break mechanism, whereas the round-nosed one does not. The difference, explained in the following list, lies on the bullet shapes:

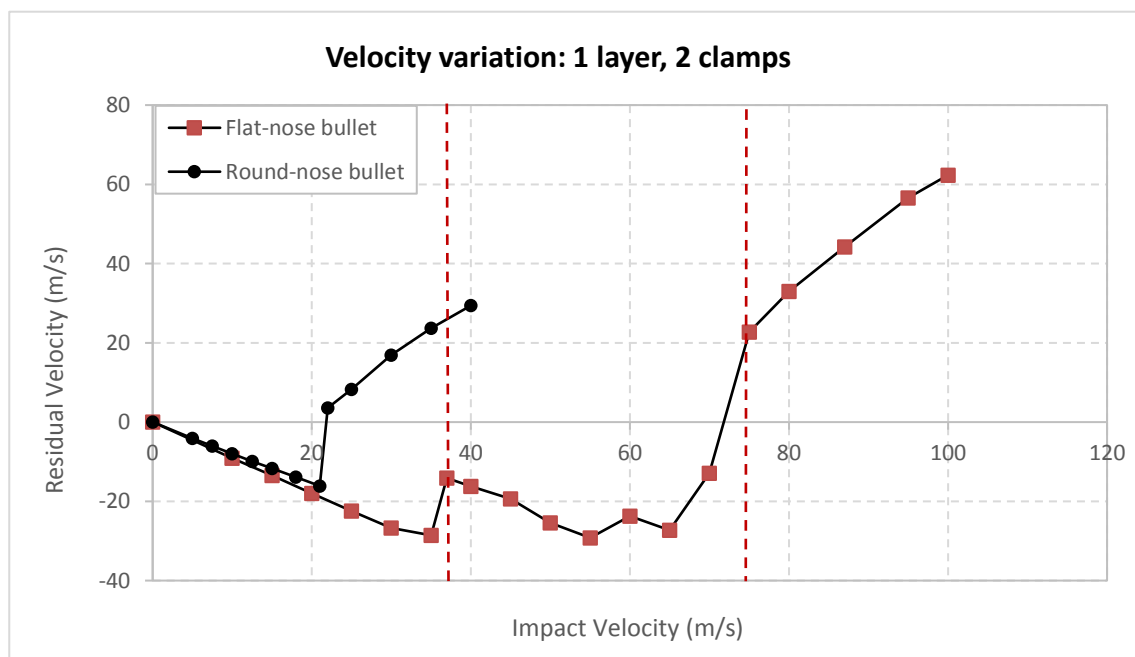


Illustration 5.16 Velocity variation after impact for flat and round cases

- a) Up to 20 m/s, the two cases behave similarly because they are working on the elastic region.

- b) For the round-nose case, push-aside mechanism and only horizontal yarns undergoing elongation provokes premature breaking (22 m/s) compared to not only the flat-nose case, but also to the reference model (40 m/s). Still, the structure of the graphic remains the same as the reference one.
- c) On the flat-nose case, the initial yarn breaking occurs at 37 m/s, being lower than the reference model. The result is expected because only half of the yarns are elongating. It can be seen comparing the energy absorption on Illustration 5.17 and the reference one on
- d) Illustration 5.6 Energy absorption comparison between flat-nose bullet and round-nose bullet
- e) . From then onwards, the yarn pull-out takes place and rises the critic velocity up to 72 m/s. This stage has been marked with red dotted lines.

Velocity variations have a direct impact on energy absorption. Illustration 5.17 reflects the importance of breaking mechanisms. While the rounded bullet only dissipates 1.8 J before breaking, the cylindrical shape reaches 17.8 J, with 14.4 J due to the pull-out effect.

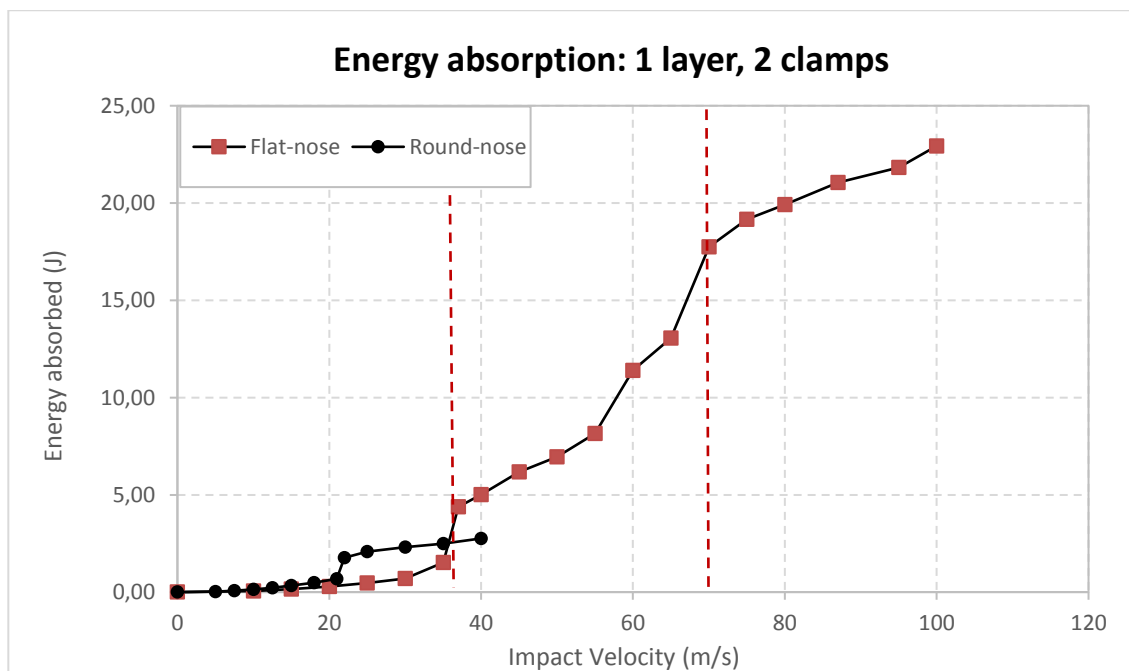


Illustration 5.17 Energy absorption comparison for flat and round cases

The values defining the trend of the curve after the breakthrough can be seen on Table 5.3.

|            | Slope<br>( $J \cdot s/m$ ) | Elasticity<br>( $\frac{\% \text{ energy variation}}{\% \text{ velocity variation}}$ ) |
|------------|----------------------------|---|
| Flat case  | 0.150                      | 0.680   |
| Round case | 0.044                      | 0.686   |

Table 5.3 Third phase curve elasticity and slope, for one layer, two-sided clamp

### 5.2.3. Two fabric layers

Adding a second layer increases the number of yarns that support the impact. Therefore, the absorbed energy should be higher than the reference experiment. The breaking mechanisms remain unmodified, as the interaction between the layers does not yield any remarkable effect visually. Thus, an equivalent analysis can be found in section 5.2.1. The impact velocities vs. residual velocities can be found in Illustration 5.18. Critic velocities have been increased from 50 to 79 m/s and from 40 to 60 m/s on the flat case and the round case, respectively.

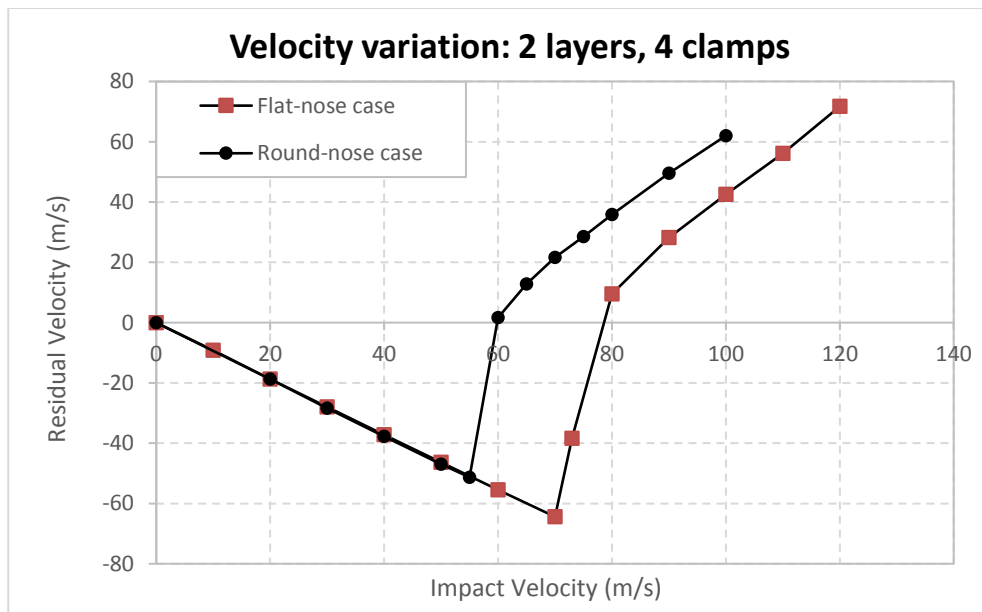


Illustration 5.18 Velocity variation after impact for flat and round cases



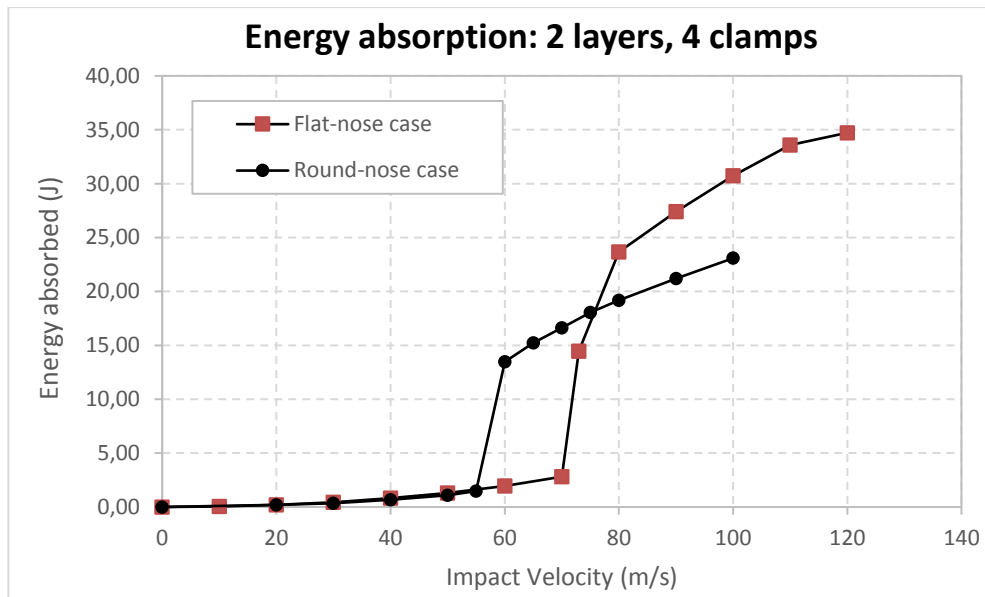


Illustration 5.19 Energy absorption comparison for flat and round cases

Regarding energy absorption, the same three stages are observed. The energy dissipation at stage two is around two times the one at the reference mode, which in general terms is an expected result. Moreover, it is slightly higher than doubled. As this is consistent for both cases, it suggests doubling the layer count yields higher yarn interaction during this phase. Table 5.4 shows trend data after the breakthrough.

|            | Slope ( $J \cdot s/m$ ) | Elasticity ( $\frac{\% \text{ energy variation}}{\% \text{ velocity variation}}$ ) |
|------------|-------------------------|--|
| Flat case  | 0.276                   | 0.934  |
| Round case | 0.239                   | 1.067  |

Table 5.4 Third phase curve elasticity and slope, for two layers

#### 5.2.4. Bullet size

For bullet size comparisons, the frontal area of both bullets has been doubled. The initial radius was modified from 4.5 mm to 6.36 mm. After the simulations, break mechanisms remain unchanged respect to the reference model. The velocity variations obtained are shown in Illustration 5.20.

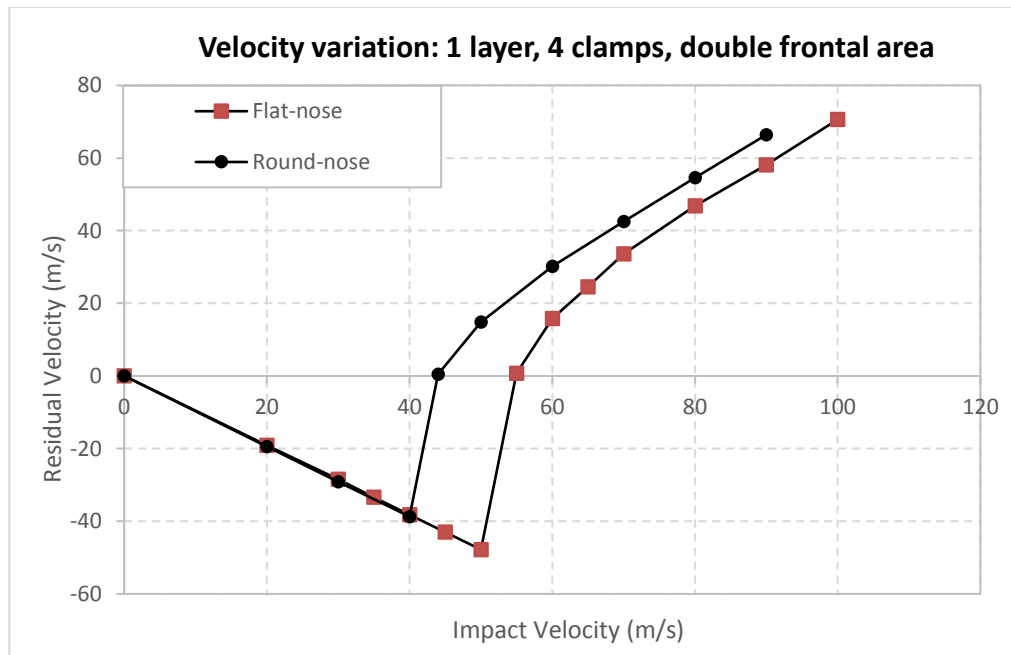


Illustration 5.20 Velocity variation after impact for flat and round cases

Nevertheless, having doubled the frontal area does not directly translate to doubled energy dissipation, but just a mere 21.1% improvement for flat-nose bullet and a 22.0% for round bullet during phase two compared to the reference case. That difference comes from velocities increasing from 50 to 55 m/s in the flat-nosed bullet, and from 40 to 44 m/s for the round-nosed bullet. The trend after the breakthrough is shown in Table 5.5.

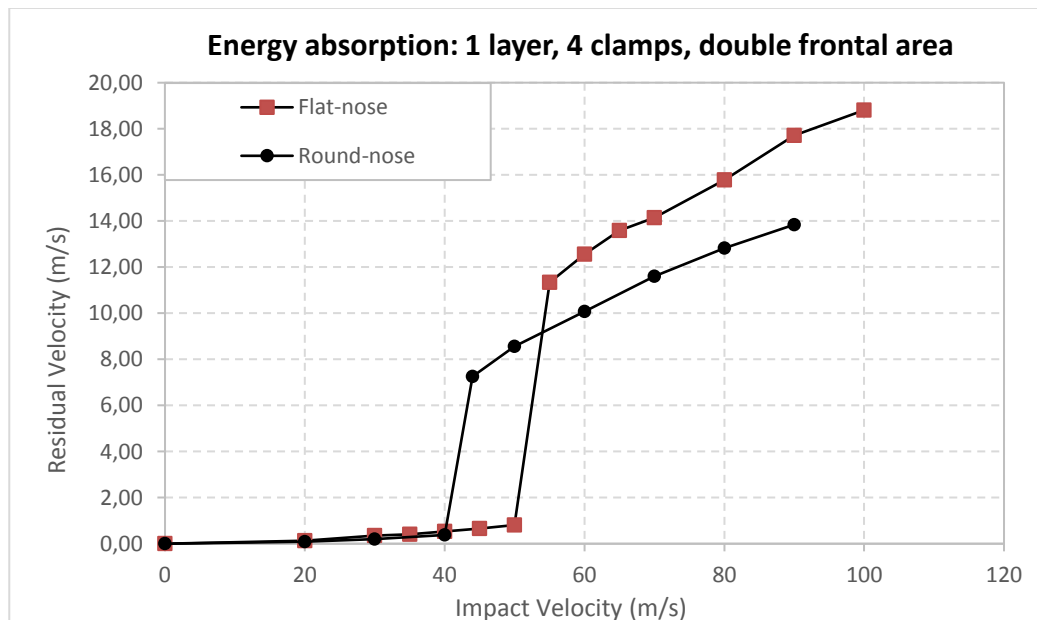


Illustration 5.21 Energy absorption comparison for flat and round cases

|                   | <b>Slope</b><br>$(J \cdot s/m)$ | <b>Elasticity</b><br>$(\frac{\% \text{ energy variation}}{\% \text{ velocity variation}})$ |
|-------------------|---------------------------------|--|
| <b>Flat case</b>  | 0.165                           | 0.804  |
| <b>Round case</b> | 0.132                           | 0.867  |

Table 5.5 Third phase curve elasticity and slope, for increased bullet size

## 6. Operating expenses

An estimation of the operating expenses is detailed on Table 6.1:

| Task   | Time (h) | Cost/time (€/h) | Cost (€)       |
|--|----------|-----------------|----------------|
| Previous literature research and understanding | 200      | 30              | 6000.0         |
| Model creation, tuning and simulation results  | 500      | 0.000125        | 5.6            |
| Of which 30% requires man hours                | 150      | 30              | 4500.0         |
| Results analysis                               | 50       | 30              | 1500.0         |
| Report writing, formatting and presentation    | 80       | 15              | 1200.0         |
| Computer 1 amortization (800 €)                |          | 0.0731          | 36.5           |
| Computer 2 amortization (900 €)                |          | 0.0822          | 41.1           |
| Abaqus licence                                 | 500      | 0.5020          | 251.0          |
| <b>Total</b>                                   |          | -               | <b>13283.3</b> |

Table 6.1 Operating expenses

Since the approach of this study is theoretical, the main contributor to the total expenses is man hours. The total amount of time invested on the project rises up to 830 hours, of which 480 require direct man involvement, representing 57.8% of the total time. Nonetheless, not all of the hours have the same consideration: literature research and problem understanding, model creation and tuning, and result analysis have a higher rating than report writing and formatting. The reasoning is based on the fact that tasks related to specific engineering knowledge should have a higher valuation.

Model creation, tuning and obtaining simulation results, require a computer constantly working during many hours. The estimated time accounts for numerous trial and error tests with the objective of learning, as well as tuning the best value for each fabric parameter. It is calculated that around 30 % of that time needs explicit user monitoring. Moreover, the use of the two computers needed to speed up the simulations should also be considered. To compute the ratio  $^{cost}/_{time}$  of each one, their price has been divided by the total life hours spent on the project, as is shown in Table 6.2.

|                                      |          |
|--------------------------------------|----------|
| <b>Years</b>                         | 10       |
| <b>Days/Year</b>                     | 365      |
| <b>Hours/Day</b>                     | 3        |
| <b>Total life hours</b>              | 10950    |
| <b>Hours spent in simulations</b>    | 500      |
| <b>Life spent on the project (%)</b> | 4.57     |
| <b>Computer 1 (€/h)</b>              | 0.073059 |
| <b>Computer 2 (€/h)</b>              | 0.082192 |

Table 6.2 Computers life expectancy and cost per hour

Abaqus expense estimate is based on the fact that yearly licence renewal for a team of five members costs at around 5000€. Nonetheless, specific deals with software vendors can notably alter this value, as well as university providing free licenses to some of their workers and students. Despite this fact, the total cost of Abaqus software once taken into account the used time only rises to 251 €, which is relatively low compared to the total cost of the project. The data used to obtain the price per hour of use is shown in Table 6.3.

|                                    |        |
|------------------------------------|--------|
| <b>Licence renewal price (€)</b>   | 5000   |
| <b>Number of people/licence</b>    | 5      |
| <b>Price/person (€)</b>            | 1000   |
| <b>Working days/year</b>           | 249    |
| <b>Working hours/day</b>           | 8      |
| <b>Number of hours of use/year</b> | 1992   |
| <b>Price/hour of use (€)</b>       | 0.5020 |

Table 6.3 Abaqus licence estimation data

Finally, the total electricity cost is computed as the multiplication of the total computing time (500 h) by the total power of both computers (90 W) and the kilowatt-hours price in Spain at the present time (0.125 €/kWh).

## 7. Conclusions and improvement proposals

The model not only produced accurate results regarding residual velocities but also successfully reproduced the expected yarn behaviors. Yarn elongation associated to fixed ends, and pull-out related to free edges as pointed out by previous literature [9], could be observed in the 1D model, as well as yarn push-aside.

Concerning to ballistic performance, the model consistently predicts lower impact velocities for the round-nosed bullet. If frontal area is increased, not much improvement is obtained in any case. On the clamping side, free ends cause pull-out, which benefits impact performance. Nonetheless, if push-aside happens, the situation is reversed and penetration occurs easier. Finally, increasing layer count consistently rises critic velocity, being a desirable option.

From these results some fabric improvements are proposed:

- a) As yarn push-aside prevents other more effective energy absorbing mechanisms, there are two suggested actions:
  - Augmenting inter-yarn friction. During the manufacturing process, fabrics can be chemically improved to obtain higher friction coefficients.
  - Yarn tightening during weaved. This measure should be further studied, as preloading the yarns may negatively affect the ballistic performance on certain circumstances.
- b) Using several layers of fabric, maximizing inter-yarn contacts if possible.
- c) If the bullets are expected to present a penetrating shape, the use of fully clamped fabrics will increase critic velocities. In case of flat-ended bullet, clamping designs that allow for yarn pull-out becomes the desired option.

## 8. Areas for further investigation

The present study has a determined scope, which can be expanded with the following ideas:

- a) Using a cohesive matrix between layers that increases load spreading.
- b) Accounting for angled impacts, which would make the model more flexible and capable of dealing with new situations. In this case, experimental data is required.
- c) Despite the actual model being successfully tested against low velocity impacts, high velocity ones are also very relevant in the field, representing a subject for future studies.
- d) The para-aramid fabric can also be tested regarding knife impacts, since body armor standards are concerned about this topic.
- e) Study natural fibers, and their performance differences with Kevlar.
- f) Analyze complex weaving and interlocks.
- g) Additionally, the actual model could also be tested on four cornering clamps. Work has already begun, as can be seen in Illustration 8.1.

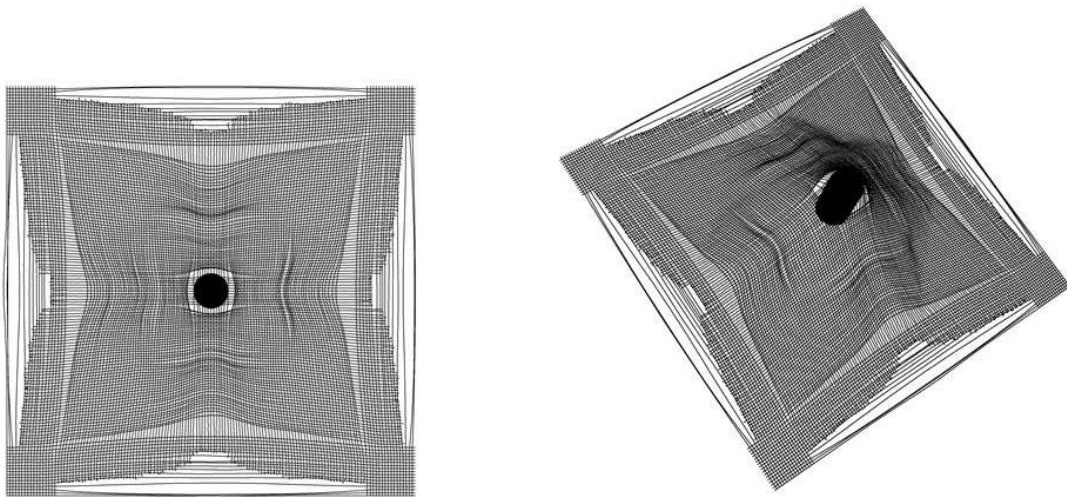


Illustration 8.1 Future investigation, four corner clamping design

## 9. Bibliography

- [1] S. Das, S. Jagan, A. Shaw, and A. Pal, "Determination of inter-yarn friction and its effect on ballistic response of para-aramid woven fabric under low velocity impact," *Composite Structures*, vol. 120, pp. 129–140, 2015.
- [2] H. H. Yang, *Kevlar aramid fiber*. Chichester: J. Wiley, 1993.
- [3] Pearce, J., 2014, "Stephanie Kwolek, Inventor of Kevlar, Is Dead at 90" New York Times. 6/21/2014, Vol. 163 Issue 56539, pB8-B8. 1/4p.
- [4] M. Cheng, W. Chen, and T. Weerasooriya, "Mechanical Properties of Kevlar® KM2 Single Fiber," *Journal of Engineering Materials and Technology*, vol. 127, no. 2, p. 197, 2005.
- [5] A., "Light in Weight, High in Performance - Kevlar® Fiber," *Kevlar® Fiber | DuPont | DuPont USA*. [Online]. Available: <http://www.dupont.com/products-and-services/fabrics-fibers-nonwovens/fibers/brands/kevlar/products/dupont-kevlar-fiber.html>. [Accessed: 11-Feb-2017].
- [6] D. Roylance, "Ballistics of Transversely Impacted Fibers," *Textile Research Journal*, vol. 47, no. 10, pp. 679–684, 1977.
- [7] Z. Li, B. Sun, and B. Gu, "FEM simulation of 3D angle-interlock woven composite under ballistic impact from unit cell approach," *Computational Materials Science*, vol. 49, no. 1, pp. 171–183, 2010.
- [8] V. Tan and T. Ching, "Computational simulation of fabric armour subjected to ballistic impacts," *International Journal of Impact Engineering*, vol. 32, no. 11, pp. 1737–1751, 2006
- [9] C. Ha-Minh, F. Boussu, T. Kanit, D. Crépin, and A. Imad, "Analysis on failure mechanisms of an interlock woven fabric under ballistic impact," *Engineering Failure Analysis*, vol. 18, no. 8, pp. 2179–2187, 2011.
- [10] G. Nilakantan, M. Keefe, T. A. Bogetti, and J. W. Gillespie, "Multiscale modeling of the impact of textile fabrics based on hybrid element analysis," *International Journal of Impact Engineering*, vol. 37, no. 10, pp. 1056–1071, 2010.
- [11] G. Nilakantan, "Filament-level modeling of Kevlar KM2 yarns for ballistic impact studies," *Composite Structures*, vol. 104, pp. 1–13, 2013.
- [12] G. Nilakantan, M. Keefe, E. D. Wetzel, T. A. Bogetti, and J. W. Gillespie, "Effect of statistical yarn tensile strength on the probabilistic impact response of woven fabrics," *Composites Science and Technology*, vol. 72, no. 2, pp. 320–329, 2012.
- [13] Y. Duan, M. Keefe, T. Bogetti, B. Cheeseman, and B. Powers, "A numerical investigation of the influence of friction on energy absorption by a high-strength fabric subjected to



ballistic impact," *International Journal of Impact Engineering*, vol. 32, no. 8, pp. 1299–1312, 2006.

[14] M. B. Mukasey, J. L. Sedgwick, D. W. Hagy, "NIJ Standard-0101.06: Ballistic Resistance of Body Armor", pp. 3-4.

## 10. Appendix

| Level            | Rigidity                    | State             | Ballistic   | Weight (g) | Velocity (m/s) |
|------------------|-----------------------------|-------------------|---|------------|----------------|
| <b>Type IIA</b>  | New                         |                   | 9 mm Full Metal Jacketed Round Nose (FMJ RN)                              | 8.0        | 373 ± 9.1      |
|                  |                             |                   | .40 S&W Full Metal Jacketed (FMJ)   | 11.7       | 352 ± 9.1      |
|                  | Conditioned                 |                   | 9 mm Full Metal Jacketed Round Nose (FMJ RN)                              | 8.0        | 355 ± 9.1      |
|                  |                             |                   | .40 S&W Full Metal Jacketed (FMJ)   | 11.7       | 325 ± 9.1      |
| <b>Type II</b>   | New                         |                   | 9 mm Full Metal Jacketed Round Nose (FMJ RN)                              | 8.0        | 398 ± 9.1      |
|                  |                             |                   | .357 Magnum Jacketed Soft Point (JSP)                                     | 10.2       | 436 ± 9.1      |
|                  | Conditioned                 |                   | 9 mm Full Metal Jacketed Round Nose (FMJ RN)                              | 8.0        | 379 ± 9.1      |
|                  |                             |                   | .357 Magnum JSP   | 10.2       | 408 ± 9.1      |
| <b>Type IIIA</b> | New                         |                   | .357 SIG FMJ Flat Nose (FN)   | 8.1        | 448 ± 9.1      |
|                  |                             |                   | .44 Magnum Semi Jacketed Hollow Point (SJHP)                              | 15.6       | 436 ± 9.1      |
|                  | Conditioned                 |                   | .357 SIG FMJ Flat Nose (FN)   | 8.1        | 430 ± 9.1      |
|                  |                             |                   | .44 Magnum SJHP   | 15.6       | 408 ± 9.1      |
| <b>Type III</b>  | Hard armor or plate inserts | Conditioned       | 7.62 mm FMJ, steel jacketed bullets (U.S. Military designation M80)       | 9.6        | 847 ± 9.1      |
|                  | Flexible armor              | New & Conditioned | 7.62 mm FMJ, steel jacketed bullets (U.S. Military designation M80)       | 9.6        | 847 ± 9.1      |
| <b>Type IV</b>   | Hard armor or plate inserts | Conditioned       | .30 caliber armor piercing (AP) bullets (U.S. Military designation M2 AP) | 10.8       | 878 ± 9.1      |
|                  | Flexible armor              | New & Conditioned | .30 caliber armor piercing (AP) bullets (U.S. Military designation M2 AP) | 10.8       | 878 ± 9.1      |
| <b>Special</b>   | Must be specified           |                   |   |            |                |

Table 10.1 NIJ Standard-0101.06: Ballistic Resistance of Body Armor [14]